LMSC/HREC A782436
HREC-11924-1

LOCKHEED MISSILES & SPACE COMPANY

HUNTSVILLE RESEARCH & ENGINEERING CENTER

HUNTSVILLE RESEARCH PARK

4800 BRADFORD DRIVE, HUNTSVILLE, ALABAMA

ELECTROFLUID CONVERTER

FINAL REPORT

25 March 1966

Contract NAS8-11924

Prepared for Astrionics Laboratory,
George C. Marshall Space Flight Center
Huntsville, Alabama

APPROVED: J. S. Farrior

J. S. Farrior
Resident Manager

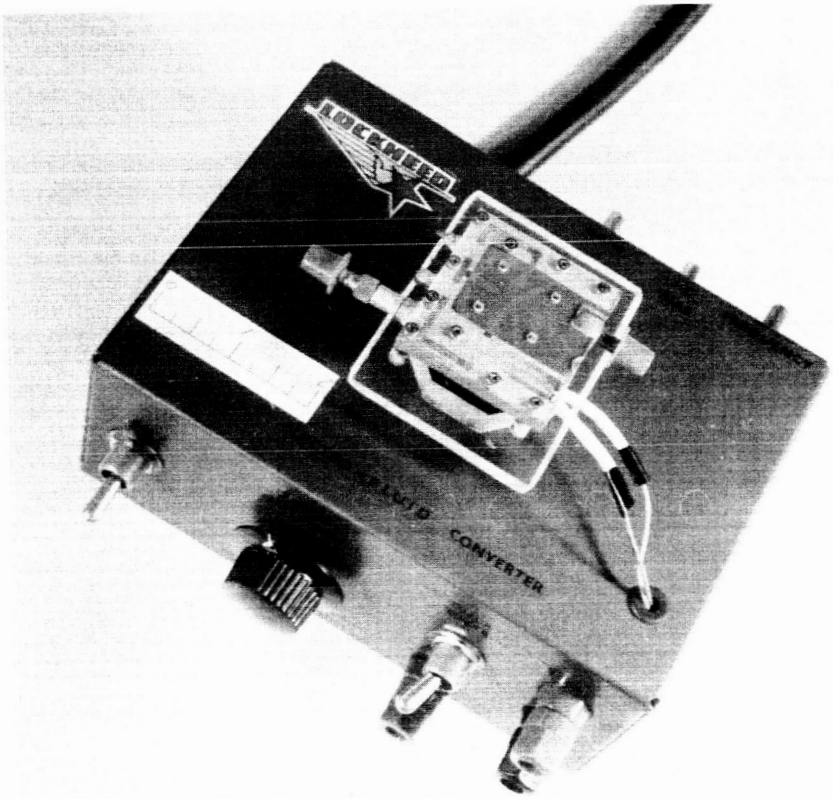

Figure 1. Electro-Fluid Converter

TABLE OF CONTENTS

		Page
	FOREWORD	
1.	INTRODUCTION	1
2.	CONCLUSIONS	3
3.	TECHNIQUES FOR CONVERSION	4
4.	METHOD OF MOTIVATION	6
5.	MODELS DEVELOPED	8
6.	COMPARISON OF MODELS	26
7.	ASSOCIATED DEVELOPMENT EFFORTS	33
8.	RECOMMENDED FUTURE WORK	39
9.	BIBLIOGRAPHY	46
	APPENDIX A: ANALYSIS OF PIEZOELECTRICAL ELEMENT MECHANICS	
	APPENDIX B: OPERATING INSTRUCTIONS, LOCKHEED/HREC ELECTRO-FLUID CONVERTER, MODEL B	

TABLE OF ILLUSTRATIONS

		Page
Fig. 1	Electrofluid Converter	Frontispiece
Fig. 2	Deflectable Splitter Test Device	9
Fig. 3	Flapper Nozzle Characteristics	10
Fig. 4	Flapper Drive Schematic	12
Fig. 5	Sensitivity vs. Static Displacement	14
Fig. 6	Model "B" Flapper Valve Electrofluid Converter	15
Fig. 7	Flapper Valve Electrofluid Converter, Model B Output Output Attenuation of Phase Shift vs. Frequency	17
Fig. 8	Acoustically Driven Electrofluid Converter Breadboard Model and Schematic	18
Fig. 9	Acoustically Driven Electrofluid Converter Frequency Response	20
Fig. 10	Voltage to Bender, Actual vs. Effective	21
Fig. 11	Manually Driven Movable Nozzle (Schematic and Photograph)	23
Fig. 12	Output vs. Deflection-Manual Movable Nozzle	24
Fig. 13	Piezoelectric Movable Nozzle Model (Schematic and Photograph)	25
Fig. 14	Diffuser Optimization Test Device	30
Fig. 15	Diffuser Static Pressure Profile for Lines of Constant Diffuser Length	32
Fig. 16	Planar Filter Type LCR Master (4_x) Schematic	34
Fig. 17	Unfiltered Pressure Output and Electrical Input vs. Time	37
Fig. 18	Comparison of LCR and "Drum" Filters	38

TABLE OF ILLUSTRATIONS
(continued)

		Page
Fig. 19	Pulse Duration Modulation, Functional Diagram	42
Fig. 20	Configuration for Time-Averaging Fluid PDM Signals	44
Fig. 21	Magnetic Motivation of Bistable Switching	45

FOREWORD

This final report documents and summarizes the results of work performed on the electrofluid converter development program, Contract NAS8-11924. This work was performed by Lockheed Huntsville Research & Engineering Center personnel for the NASA Astrionics Laboratory of the George C. Marshall Space Flight Center during the period June 25, 1965 to March 25, 1966.

Various electrofluid converter concepts were developed and models demonstrating each concept were fabricated and investigated. The converter is required to be suitable for driving a proportional pure fluid amplifier. The program included identification of techniques, component analysis and simulation, hardware development, elementary laboratory experiments, and developmental model fabrication test, demonstration, and delivery.

Principal contributors on this program were Dr. C. S. Chang, Dr. W. Trautwein, G. O. Floyd, P. R. Bradie, T. Dannback, R. B. Fuller, and J. E. Reich. NASA/MSFC Technical Supervisors for the contract were Messrs. W. L. Howard, J. R. Smith, C. S. Corneilus, and J. A. Peoples of the Flight Control Development Branch, Astrionics Laboratory.

1. INTRODUCTION

Although pure fluid devices have found wide application for sensing, switching, amplification, controlling, and computation, within any given system it is often desirable to perform part of the system functions electronically. In such a part-fluid, part-electronic system, it is necessary to perform the signal conversion from electric to fluid. Such an electric-to-fluid interface device is the subject of this program. The conceptual studies and developmental activities associated with this effort resulted in three successful models employing piezoelectric benders as conversion mechanisms. One of these models, a flapper valve type, was refined into an integrated package.

Two distinct methods of accomplishing electric to fluid conversion were investigated. One method involves deflection of the fluid flow (stream) by fluidic means, and the other achieves the required conversion by electromechanical actuation. Motivation techniques considered include piezoelectric means, magnetostrictive devices, and control by reed deflection. Each of these techniques is capable of receiving an electrical input and converting it into a mechanical or pressure output to cause changes in fluid flow. The piezoelectric method of motivation was the one explored on this program.

Related areas, such as design and development of a pneumatic filter, reduction of time delay in converters, and flow visualization, which are common to all models, were investigated in various degrees. Methods of signal conversion were also thoroughly evaluated.

Four electrofluid converter concepts were considered and investigated: (1) deflectable splitter; (2) flapper valve; (3) acoustic driver; and (4) movable nozzle. Models of each were built, compared and evaluated.

The most promising one, the flapper valve concept, was selected and development work was continued to improve the performance characteristics of this selected model.

2. CONCLUSIONS

As a result of the work performed under this contract by Lockheed Missiles & Space Company's Huntsville Research & Engineering Center, the following conclusions are determined:

1. Small, light-weight, high performance electrofluid converters are feasible. Four electrofluid converter model types, (1) the flapper valve, (2) the acoustical driver, (3) the movable nozzle, and (4) the deflectable splitter, were fabricated and tested. Types (1), (2), and (3) were successfully demonstrated.

2. The design of the flapper valve model was refined to improve its performance. All components of the model were integrally packaged to reduce the size of this converter.

3. Modulation and control of fluidic devices through the use of piezoelectric elements were successfully accomplished.

4. The movable nozzle electrofluid converter shows excellent potential for an alternating input operation but it does not perform well in the direct or constant level input mode.

5. Special test devices, namely, the diffuser optimization test device and particularly the manually movable nozzle test device, were successfully used for preliminary determination of design data.

3. TECHNIQUES FOR CONVERSION

In the initial phase of this development program, several electrofluid conversion techniques were considered. The most promising technique involves deflecting a fluid stream. In addition, a technique of throttling a fluid stream, so that the downstream pressure changes as a function of the input electrical signal, was developed.

In the beginning of this project, it was realized that rather weak signal energies would be employed in the converter. Use of the throttling process requires an additional amount of energy because of the energy losses in the conversion. Fluid stream deflection does not have this drawback. When a fluid stream is deflected without inducing turbulence or rotational flow, the entropy of the stream remains constant. The energy level for deflection is low compared to the energy within the fluid stream itself. Consequently, it was determined that electrofluid conversion could best be accomplished by using the throttling process for controlling the conversion, and stream deflection would be used to provide amplification to compensate for energy losses.

First, the area of magnetohydrodynamics was given a cursory study for possible applicability, but the study was discontinued because the phenomena within this field required an electrically-conductive fluid. Second, the application of thermal energy was considered but discarded; long response times are inherent within a thermally excited system. This study lead to selecting techniques of conversion involving stream deflection by use of fluids and by use of mechanisms.

Stream Deflection by Flueric Means

Two methods of deflecting the stream by flueric means are: (1) establishing a pressure inbalance across the stream; or (2) by adding momentum at right angles to the fluid stream. The main drawback of these methods are that some stream energy is lost when establishing a pressure inbalance or that energy must be added to give increased momentum. However, in the latter case, a sufficient quantity of energy is recovered within the jet stream. This method becomes most desirable if an adequate means of motivation can be developed.

Stream Deflection by Mechanisms

Mechanical intervention requires a relative high order of power, in comparison with stream deflection methods by fluerics, to move both the element and the stream. The method of motivating these techniques of conversion was then considered.

4. METHOD OF MOTIVATION

Initially, a method for gaining pressure imbalance by a high-energy spark was investigated but proved undesirable since this method had problems of high voltage, radio-frequency interference, and possible thermal degradation of materials. Momentum addition, pressure imbalance and mechanical intervention required the conversion of electrical energy to mechanical motion before fluidic energy could be derived.

Conversion of electrical to mechanical energy can be accomplished by utilizing established fields of electrical or magnetic flux. The most common applications of magnetic flux, motors and linear or rotational solenoids, were ruled out because high relative sliding speeds between mechanical members decrease the reliability and increase the energy requirements. Mechanical energy can be gained by magnetic flux fields as in magnetic reed control, magnetostrictive devices, and by electrical flux fields in piezoelectrical devices.

Magnetic Reed Control

The operation of these devices is based on a flexible cantilevered beam, made of some ferromagnetic material, being deflected by the influence of an electromagnet. If the reed is mounted in a fluid amplifier and deflected by the magnet the jet stream, being attached to the reed by the Coanda effect, will then be deflected with the reed.

Some deficiencies soon become apparent: (1) these devices are highly non-linear, since magnetic attraction forces are inversely proportional to the square of the distances over which the force must extend; (2) the inverse square law by which these devices are limited leads to large hysteresis in dc operation. Because of these deficiencies, these devices did not warrant further development.

Magnetostrictive: These devices are made from a metal, usually a nickel alloy, with an anisotropic crystalline structure that deforms in the presence of a magnetic flux field. This crystalline deformation results in a dimensional change along some preferential axis, and may be either negative (magnetostrictive) or positive (magnetoexpansive). These dimensional changes develop extremely high mechanical forces and, excluding the effects of inductive heating, result in a very high efficiency of energy conversion. However, the magnitudes of the coefficients of thermal expansivity and magnetostriction are almost the same. The microinches of dimensional changes brought about by impressment of a magnetic field are insignificant in comparison to the large changes brought about by variations in ambient temperature. These devices were excluded from this developmental effort because of their thermal sensitivity relative to their application for electrofluid conversion.

Piezoelectric: These devices are made from a compacted crystalline mass, usually a ceramic of metallic oxides, whose crystalline structure deforms in the presence of a field of electrical potential or, conversely, will develop an electrical potential when mechanically deflected. Rochelle salts, used in phonograph cartridges, are an excellent example of piezoelectric material. Piezoelectric material is thermally stable, and has a very high coefficient of piezoelectric deformation when compared with their coefficient of thermal expansivity. They maintain their piezoelectric characteristics up to their Curie temperature, which may be as high as 365°F.

Dimensional changes caused by piezoelectric behavior is in the order of microinches. However, a class of piezoelectric devices have been made where two piezoelectric ceramic strips have been bonded to a flexible member. For any given electrical field potential impressed across these pieces, one side will expand while the other contracts. The relative dimensional changes are magnified in the same manner as a bimetallic strip used in a thermostat. With a simple cantilevered beam arrangement, motion at the tip is on the order of many thousandths of an inch. When a potential field is cyclically impressed at the resonant frequency of the piezoelectric beam, the amplitude at the tip is increased over that of simple dc operation. Another positive characteristic of ac operation is that amplitude, at resonance, is directly proportional to the strength of the impressed electrical field. We decided to develop models that had piezoelectric devices for electrofluidic motivation because of all the positive factors evidenced by these devices.

5. MODELS DEVELOPED

Deflectable Splitter

The first model considered for development is a "deflectable splitter" device. The features of this device, which utilizes electromechanical mechanisms as a method of conversion, are discussed below.

In a conventional, planar, proportional, pure-fluid amplifier, if the splitter is hinged for deflection (similar to an airplane control surface), it is capable of controlling the fluid stream direction. Such a deflection is small and the splitter can be driven by any convenient motor device. A test model was designed and fabricated to study this concept. In the test device for experimentation purposes a long lever arm was utilized to manually deflect the hinged splitter (Figure 2). In addition, small variations in receiver width and location were possible by providing for the capability of adjusting the outer walls of the receiver. Operational tests were then run to determine the useful range of splitter deflection and the resulting changes in fluid direction and output.

Preliminary tests conducted with the test device were not conclusive. The power jet attaches itself to the splitter due to Coanda effect and does not detach for small angular deflections. Indications are that if the splitter is rotated sufficiently to detach the stream, rotational flow in the form of a vortex sheet develops downstream, thereby resulting in high power losses. Also, the characteristics of jet attachment result in a large hysteresis for the device. Therefore, the deflectable splitter concept was held in abeyance until some means of flow visualization is developed to investigate flow attachment/detachment.

Flapper Valve

The next concept considered for investigation is a flapper valve/nozzle arrangement wherein the flapper is controlled by an electrical input and the output goes to a control port of a proportional fluid amplifier.

Flapper-nozzle configurations have been used extensively in many fluid devices. The usual technique is to vary the pilot, or upstream, pressure at the nozzle mouth by movement of the flapper. A different approach is used in this application. A flat plate (flapper) pressed solidly against a nozzle will completely stop the flow. If the plate is moved away from the mouth of the nozzle, the flow increases as the distance, L, increases (Figure 3). However, each outward increment of distance, L, has less and less effect on the flow rate from the nozzle until a point is reached where additional outward movement of the plate has no further effect. When the flapper is located at a stand-off distance, or "zero" point, some distance from the mouth of the nozzle and then oscillated, the average flow during one cycle of oscillation

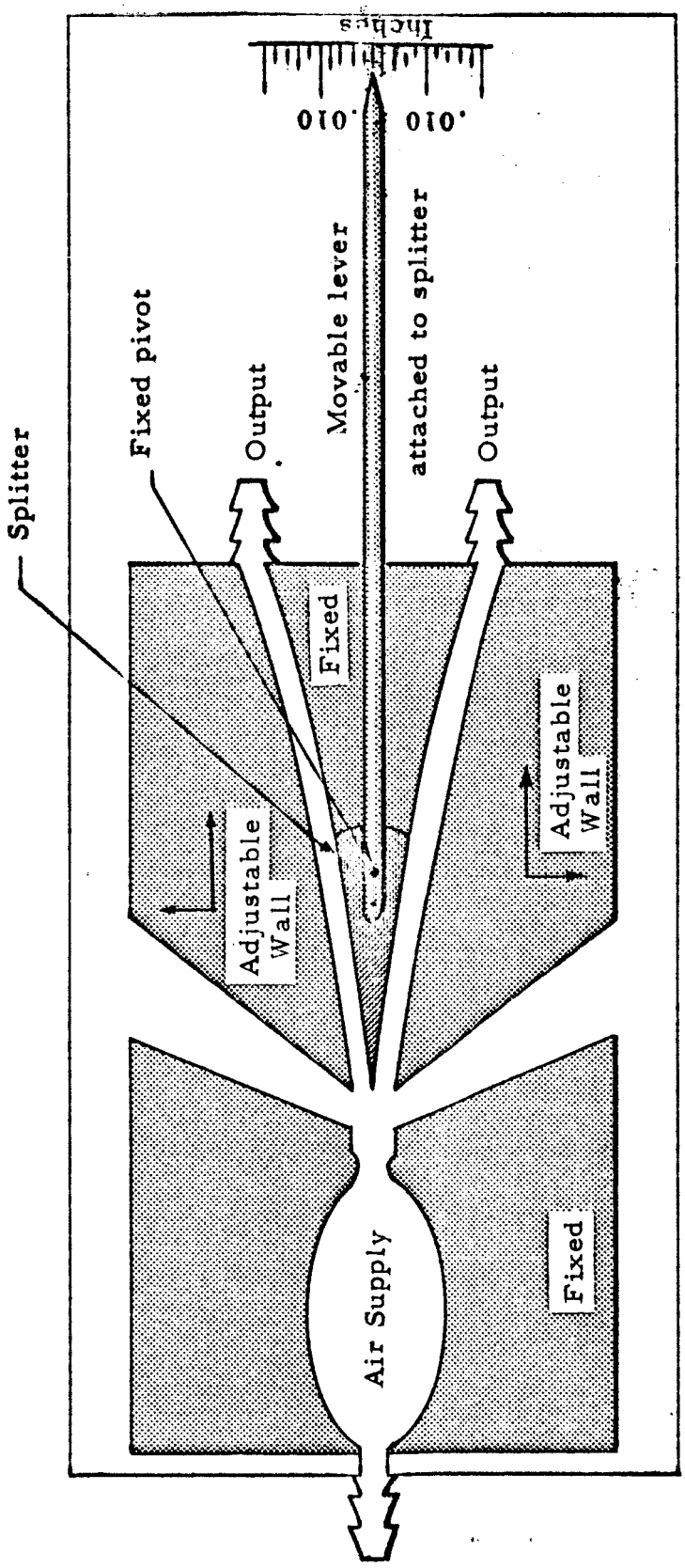

Figure 2 - Deflectable Splitter Test Device

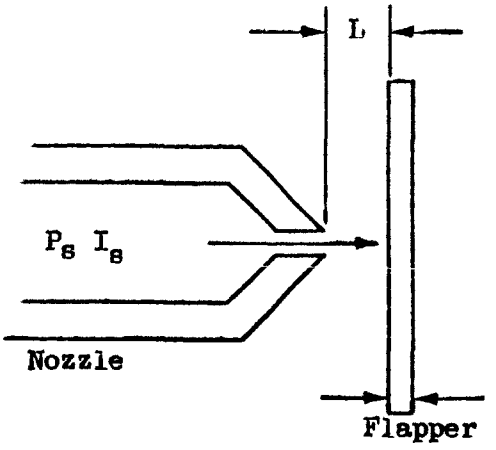

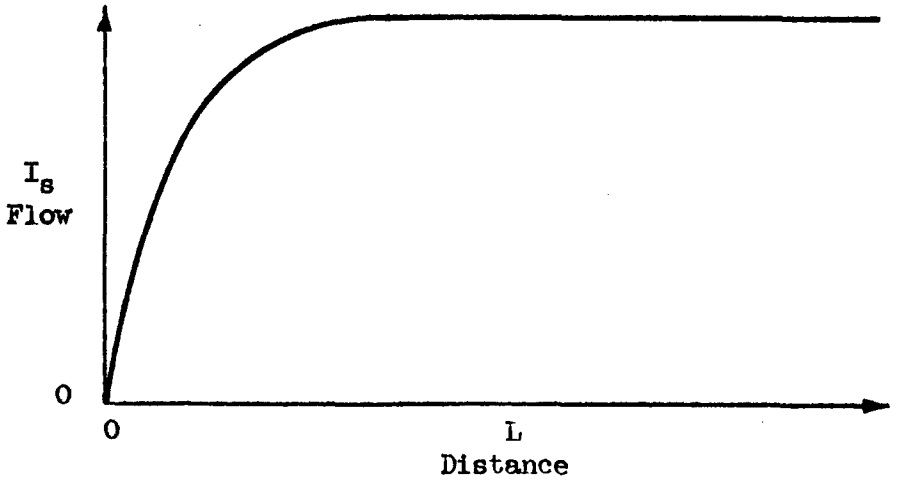

Figure 3 - Flapper Nozzle Characteristics

is directly a function of the amplitude of the oscillation. The average flow decreases from the value at the "zero" point of the flapper as the amplitude of oscillation is increased. This result is related to the shape of the curve shown in Figure 3. The slope of the curve is steeper for one half of the flapper cycle than the other half and, consequently, the average flow rate over a cycle is lower than the flow rate when the flapper is stationary at the zero point. When the flapper is inserted within a cavity in such a manner that nozzle output flow enters the cavity, then increasing the amplitude of oscillation of the flapper results in a decrease in the integrated flow into the cavity. The cavity exits into a control port of a proportional fluid amplifier. A bias pressure and flow is maintained on the opposite control port. The power stream of the proportional fluid amplifier exits through a side vent at zero flapper amplitude, and progressively moves toward and through the adjacent output leg as flapper amplitude increases. The jet stream is entirely directed toward the output leg at maximum flapper amplitude (maximum pressure output).

A piezoelectric bender is used as the material for the flapper and it responds quite satisfactorily to being driven with an alternating voltage source. The force tending to push the flapper away from the nozzle is relatively large in comparison to the mechanical force generated by a piezoelectric bender. If the piezoelectric bender is placed flush with the nozzle and then electrically driven, only half of the cycle is effective, free resonance is precluded, and the highly directional forces lead to early failure of the bender. The present usage of the flapper is a preferred application, where the constraints, due to the piezoelectric material, are taken into consideration. Analysis of piezoelectric mechanics is given in Appendix A.

The electronics package for supplying power to the piezoelectric bender in the flapper valve model consists of (1) an oscillator; (2) a modulator; (3) a voltage amplifier; and (4) a power amplifier for driving a voltage step-up transformer, as shown schematically in Figure 4.

The oscillator is an astable multivibrator. Since the oscillator frequency is at the resonant frequency of the crystal, an applied square wave, which works as well as a sine wave and is easier to produce, control and modulate, is used. Modulation is accomplished by simple diode clipping of the oscillator square wave. This unit produces up to 250 volts p - p across the crystal. To achieve this voltage, coupling with a commercial, laminated transformer is used in the test model. For a flight item, a powdered iron transformer is most likely to be used.

The modulated input signal is in the 1 volt maximum p - p range. A two-stage amplifier is used to boost this to 20 volts maximum p - p, and the transformer then raises this to over 200 volts maximum. An emitter follower output stage delivers up to 4 watts of power to the transformer which in turn delivers up to 40 milliwatts to the crystal.

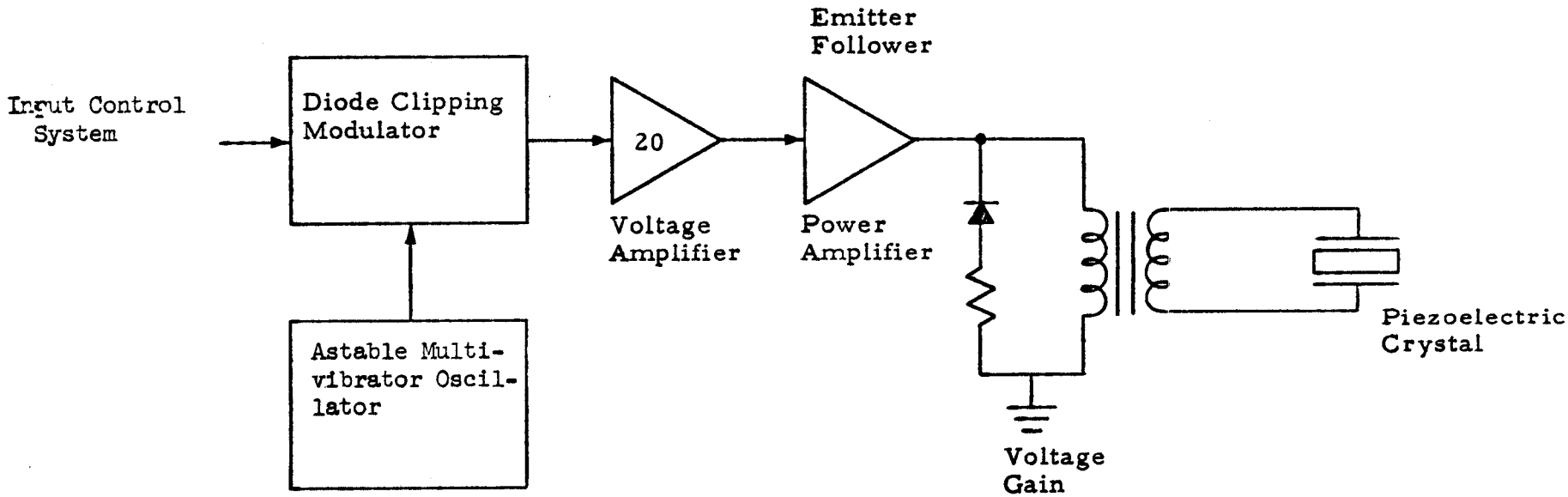

Figure 4 - Flapper Drive Schematic

Tests were run on various nozzle and flapper plate shapes to establish validity of basic principles. The sensitivity of the flapper-nozzle configuration to static distance setting at a 3 psig supply pressure is shown in Figure 5.

At first, several open-type (Model A) units were built, then an enclosed Model B was designed and built, both types using piezoelectric benders (flappers). The closed-type Model B performed far better than the open-type model. Only two most advanced versions of Models A and B will be discussed.

Model A: The Model A flapper valve electrofluid converter was subjected to closed-loop testing. Closed-loop negative feedback was accomplished by sensing the converter's output with a pressure transducer and summing this voltage with the converter's input signal with a dc amplifier. A forward loop gain of 20 was maintained in the closed-loop operation. Thus, attenuation of input signal and converter non-linearity of output signals were greatly reduced while time response was improved.

Model B: The advanced Model B is a semi-integrated package which includes a fluid amplifier coupled to the flapper valve (see Figure 6). Major improvements over Model A were in packaging, sealing, power requirements (both electrical and fluidic), and frequency response.

The semi-integration of Model B not only enhanced size and appearance, but greatly improved performance (as shown in Table I, Section 5) by reducing channel lengths and facilitating good sealing. This model was designed for single planar etching, although the one actually built was milled from aluminum. The milled model has cavities in place of the flapper valve and fluid amplifier. These cavities permit three different amplifiers to be tested in the package instead of one, if it had been integrally made. The planar etching technique will permit simple fabrication of an integral package in which only the piezoelectric element and its associated wedges and spacers must be installed.

In the Model B, the flapper valve unit was designed in the smallest size which could deliver full control power to a common fluid amplifier. A compatible fluid amplifier was selected and set to operate in a region that gives the best converter input sensitivity and minimum fluid power requirements.

The flapper valve unit's input orifice diameter was set a 0.018 inch, supply pressure 3.5 psig, and the output orifice diameter 0.040 inch. A shorter bender increases the resonant frequency to 1120 Hertz. Effectiveness of the new flapper valve increased the ratio of flow change to average flow, resulting in an output signal-to-noise ratio of 25:1 compared to the Model A's 10:1.

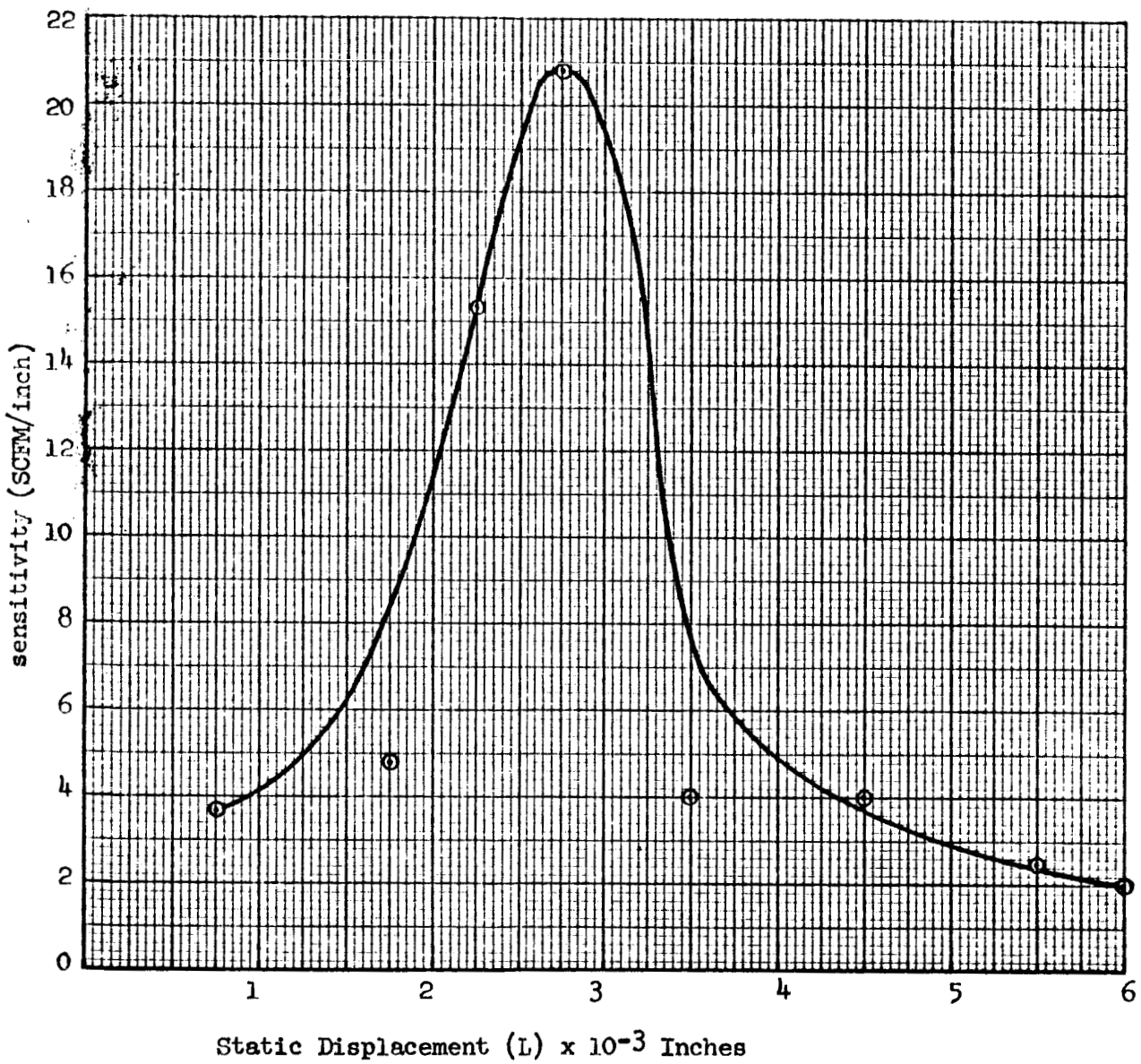

Figure 5. Sensitivity vs. Static Displacement

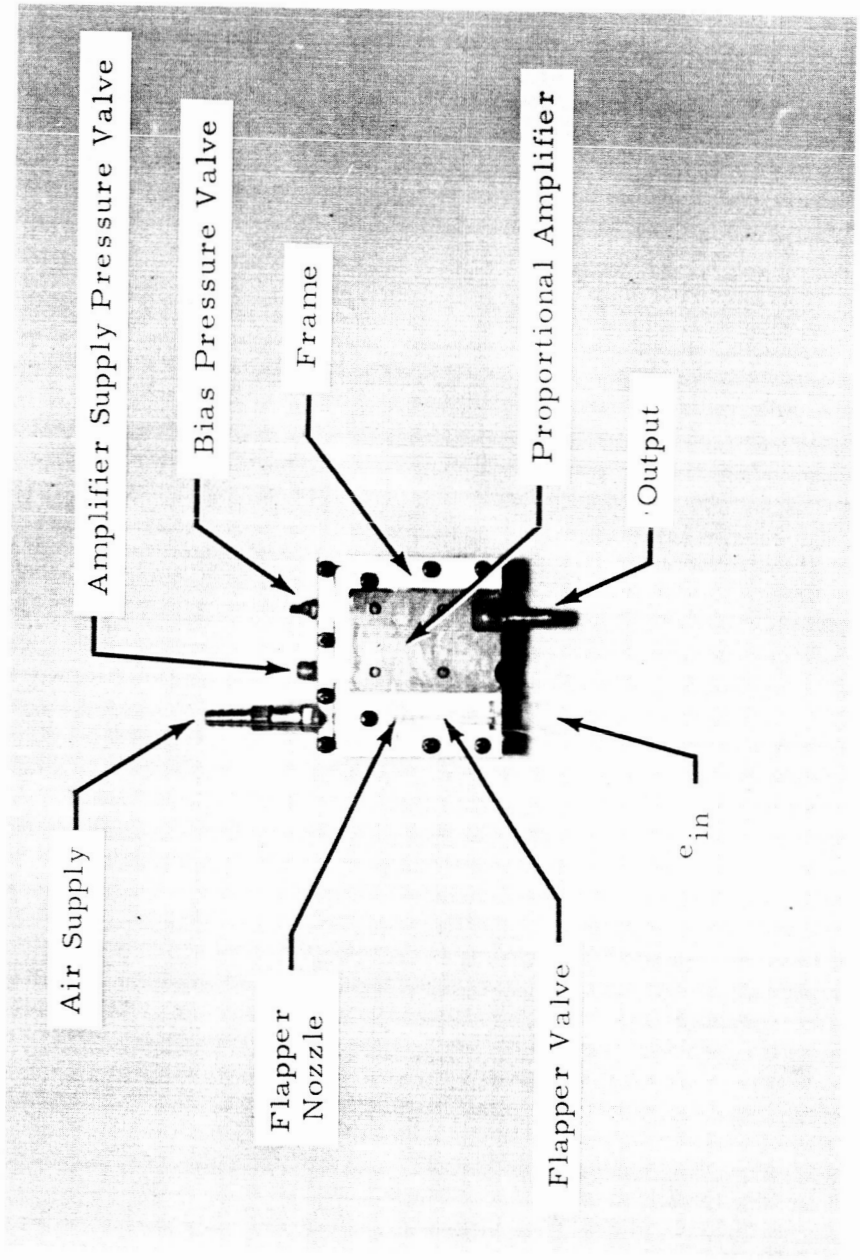

Figure 6 - Model "B" Flapper Valve Electrofluid Converter

Electrical power to the bender is small since the bender is essentially a capacitor. Therefore, the smaller crystal in Model B offers no appreciable electrical advantage over larger crystals. Maximum excursion of the flapper valve must remain within 0.020 inch; these physical limits and the fluid pressure of 3.5 psig to the flapper valve input orifice establish the electrical requirement of 80 volts rms for the given bender. Bender dimensions are: thickness 0.021 inch, length 0.875 inch, width 0.085 inch, and a cantilever arm of 0.53 inch. The bender excursion limit must be large enough to maintain a high flueric output signal, yet low enough to avoid excessive voltage requirements.

Frequency response of the Model B was greatly improved over that of the Model A largely because of the semi-integration of the package. The improved packaging reduced the critical channel length between flapper valve exit and amplifier control port from 1.5 down to 0.7 inches. Reduction of dead space around the flapper further improved frequency response, since the extra volume was providing space for storing air (analogous to a capacitor storing a charge). Frequency response of the Model B converter with the drum filter (see Section 7 for drum filter) is given in Figure 7. The transfer function was derived empirically from the data to approximate the curve.

Acoustic Driver

Experience gained from the flapper valve converter indicates that if a standard proportional amplifier is biased to near cut-off at one control port, it will practically rectify an ac pressure applied to the opposite control port. The amplifier can be biased for extreme sensitivity to small control signal changes. This combination of rectification and sensitivity leads to the concept of driving an amplifier with acoustic pressure pulses from a device similar to a common loudspeaker. The acoustically-driven electrofluid converter system, shown in Figure 8, is composed of three elements: the acoustic driver, a rectifying amplifier, and a power amplifier. The first stage amplifier, a center-dump proportional amplifier, is operated without control pressure bias and with one output leg blocked. Only the positive acoustic signal is amplified and accepted as output, thereby accomplishing rectification. The unused output side is blocked, which builds up cavity pressure and gives effectively a positive feedback from the unused output side. The second stage amplifier, the power amplifier, is a biased, proportional amplifier and is used to boost the level of output signal. The entire system uses a common air supply at 3 psig which, in turn, is reduced through needle valves to the proper pressures for the first stage amplifier supply and the second stage control bias.

The acoustic driver is a cantilevered strip of piezoelectric bender set within a small cavity and allowed to freely resonate. The bender is excited by an ac carrier signal with a frequency corresponding identically to the resonant frequency of the bender. The displacement of the resonating bender is then proportional to the rms amplitude of the ac signal that is over the beam's threshold voltage. The acoustic pressure output is, in turn, proportional to the beam displacement and ac signal amplitude. Earlier tests, using amplitude modulation in the Model A electrofluid converter, indicated an improved time response was obtained for the device by using a small resonant

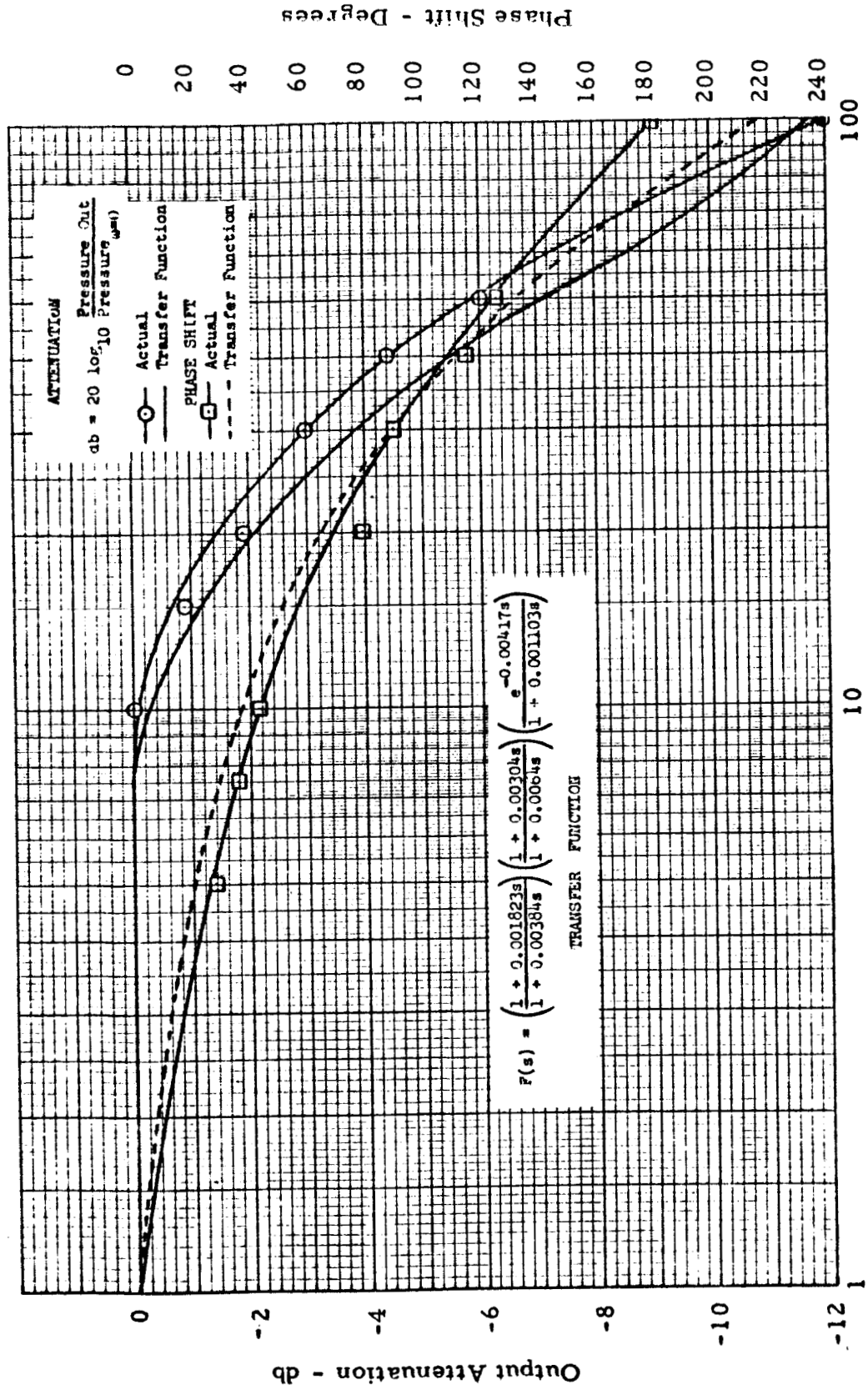

Figure 7 - Flapper Valve Electrofluid Converter, Model B
Output Attenuation & Phase Shift vs Frequency

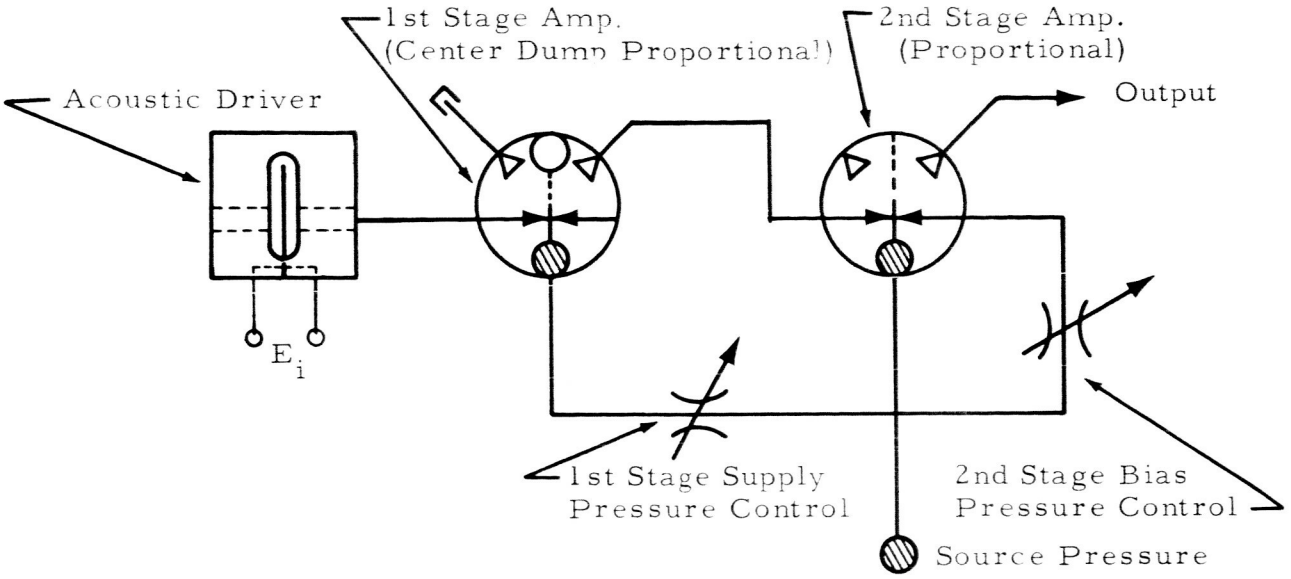

Converter Circuit

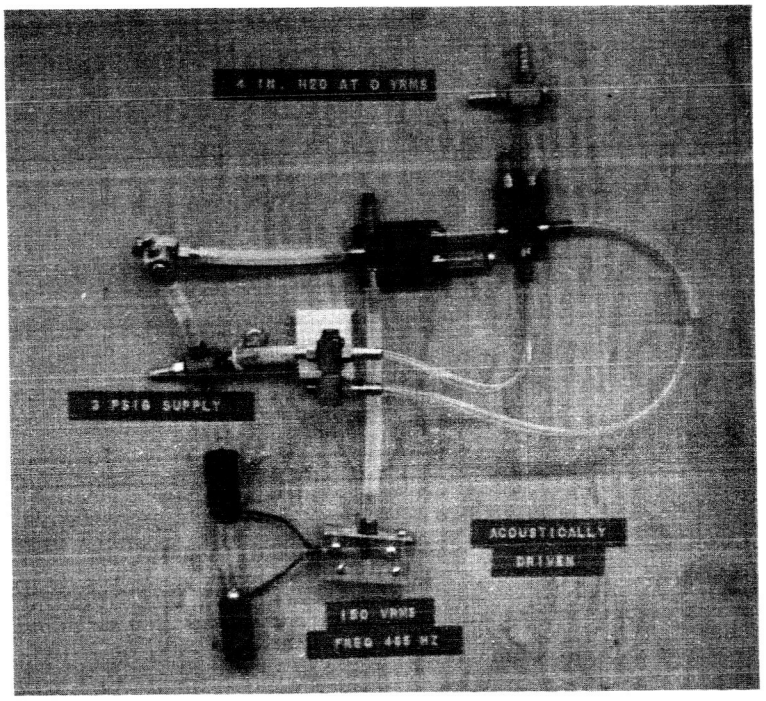

Figure 8 - Acoustically Driven Electrofluid Converter Breadboard Model & Schematic

member to obtain a higher resonant frequency. Power output is proportional to beam deflection, or beam length, but a longer beam has a lower resonant frequency. On the acoustic model, a compromise was reached between the driving power and the frequency response requirements to determine the beam's best operating frequency. A maximum swing of $\pm$ 0.030 inch at 465 Hz was used. The cavity is sized so that the swept volume of the resonating beam is approximately one half of the total cavity. Output pressure is directly a function of the ratio of swept to total volume, but the increased complexity of fabricating a cavity for a volume ratio close to unity was not considered warranted at this time. Present output from the acoustic driver at 150 volts rms (maximum input) is a sinusoidal pressure wave at 0.2 inches of water and essentially zero flow.

Output signals from the acoustic driver are then passed through the first stage amplifier where it is rectified and amplified by a factor of five. Output from the first stage amplifier is a dc signal of 17 inches of water with the rectified and amplified acoustic signal imposed upon it. This signal enters the second stage (power) amplifier where the dc signal is almost completely biased out.

Biasing the second stage amplifier serves two purposes. Primarily, it removes the dc component from the first stage output, and, secondarily, it increases the sensitivity of the second stage, raising the amplification from a nominal value of 5 to 7. The second stage amplifier output was loaded with an orifice 0.013 inches in diameter to simulate an additional fluid component located downstream. With this loading the output of the second stage amplifier was 4 inches of water at zero system input and 11 rms inches of water at maximum system input. The rectified carrier signal appears as a sinusoidal wave of 232.5 Hz imposed on the dc signal. Peak-to-peak amplitude of the ac signal is almost equal to the dc level. A low-pass filter circuit was developed to eliminate the high frequency noise over 1 KHz in the system and reduce the ac signal component.

The low-pass filter, which is employed with the acoustically-driven electrofluid converter and is tuned for the converter, reduces the noise level to within 1% of dc level; and reduces carrier amplitude, at maximum signal, to a 5% ripple on the dc signal. However, large volumes and long lengths within the filter circuit adversely affect the dynamic response of the converter system. A power loss of three decibels occurs at a frequency of 0.17 Hz, and the corresponding phase shift is -43 degrees. System time delay is approximately 0.11 seconds, with the major portion of this caused by the filter circuit.

Frequency response data are presented graphically in Figure 9. Frequency response tests were run by modulating the carrier frequency amplitude between 0 and 300 rms volts. The piezoelectric bender threshold is 100 rms volts, so the effective signal to the acoustic drive appears as a clipped sine wave with only the portion between 100 and 300 rms volts usable, as shown in Figure 10. A full third of the input is thus lost before the bender starts to respond. The characteristics of the frequency response curve indicate the

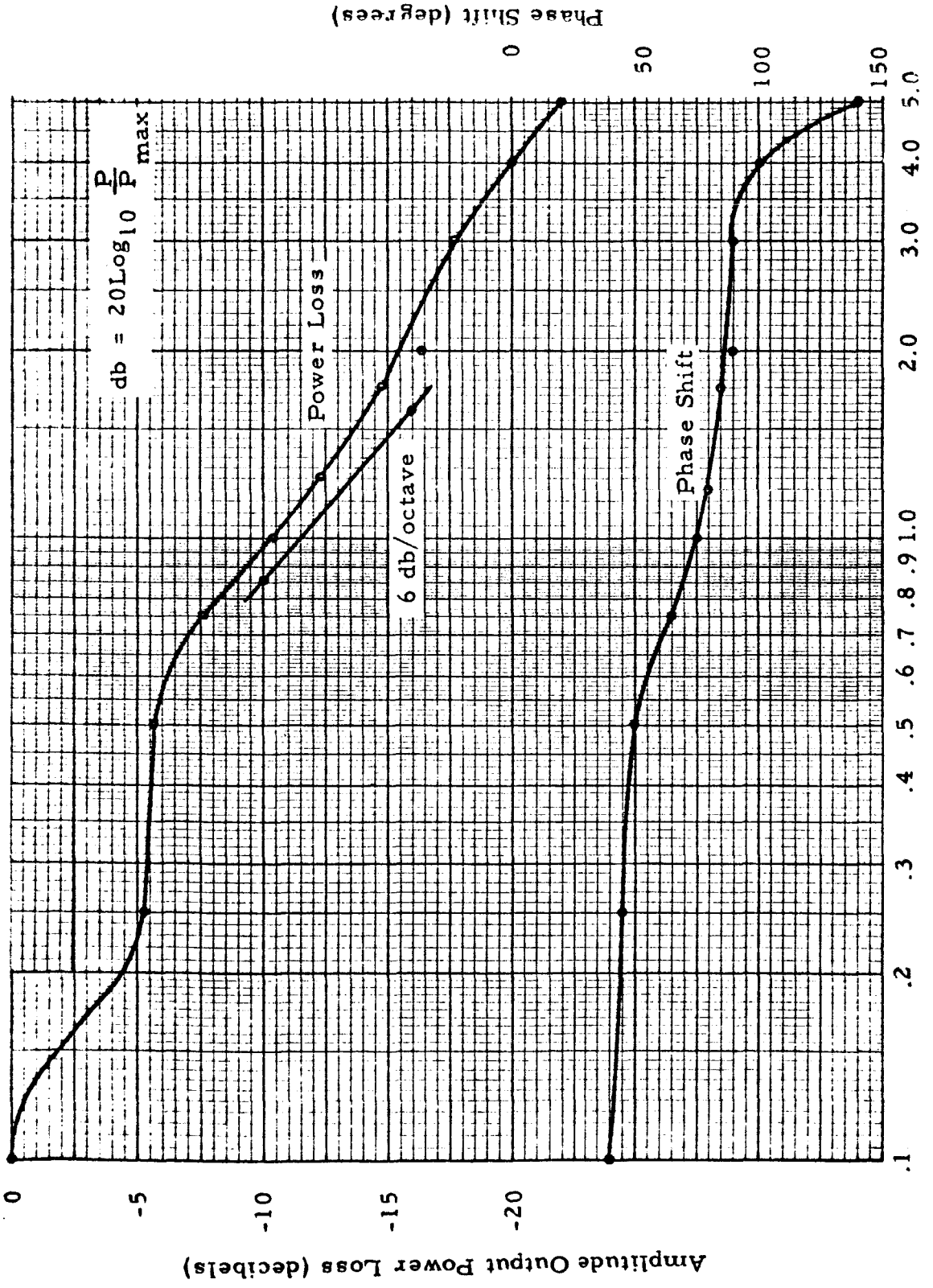

Figure 9 - Acoustically Driven Electrofluid Converter Frequency Response

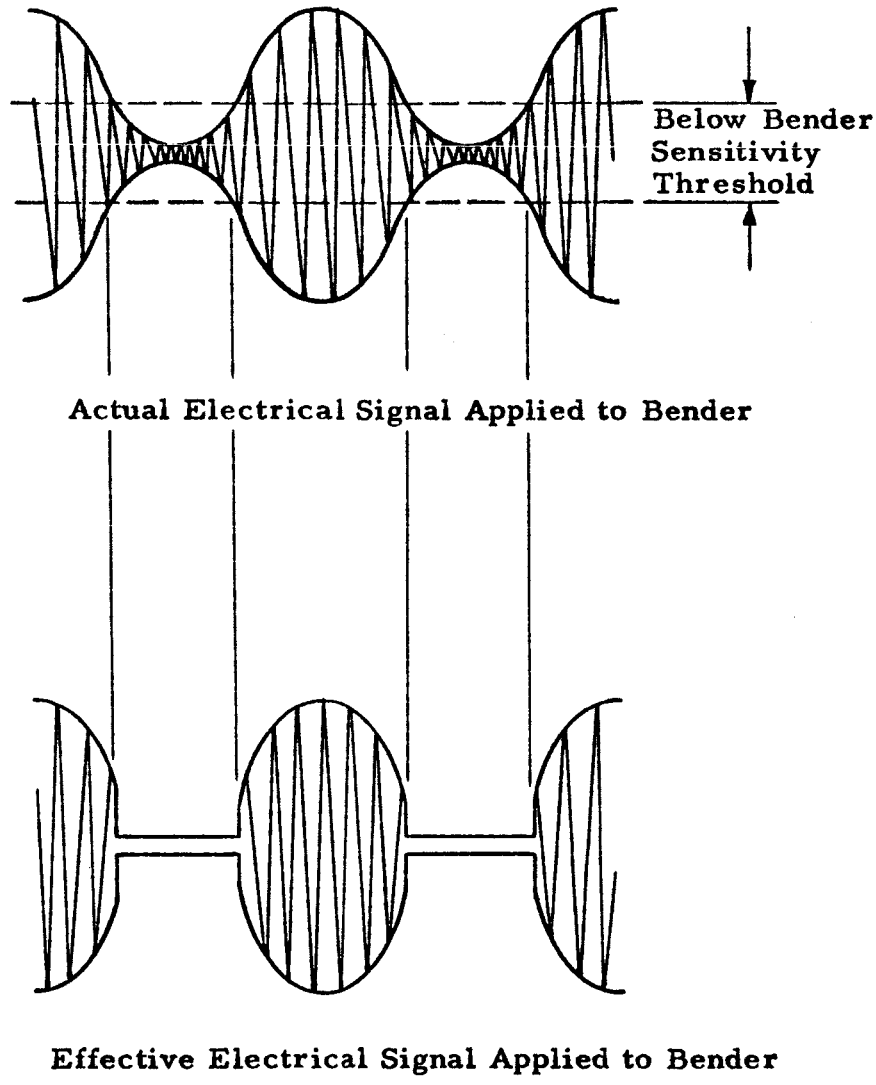

Figure 10 - Voltage to Bender, Actual Vs. Effective

true behavior of the converter system. The initial power loss below 0.6 Hz follows the approximate slope of -6 db/octave characteristic of a simple, first-order system. Phase shift also remains essentially constant to about 0.6 Hz. This behavior is a strong indication that the initial rolloff is erroneous and that the error can be caused by the input being clipped (bender threshold) modulation. With the initial ac bias being equal to the bender threshold voltage, system behavior can be closely approximated by:

$$\frac{P_o}{E_i} = \frac{e^{-0.11s}}{1 + 0.2655\,s}$$

The above equation can be derived from the frequency and phase response data shown in Figure 9.

Movable Nozzle

If a proportional fluid amplifier is cleanly severed between its supply nozzle and receiver, it is possible to control the percentage of supply stream diverted to each receiver by manipulating the supply nozzle. The movable nozzle model (Figure 11) is built from commercially available fluid amplifiers and a specially made test fixture for mounting the severed parts along a common plane. The test fixture permits a range of locations for the severed parts relative to the movable nozzle pivot point. The movable nozzle can, thereby, be set for pure rotation or practically pure translation. Tests were run in the range of physical situations attainable in the planned, piezoelectrically-motivated movable nozzle. The output of the model for various values of "L", the splitter distance from the throat of the amplifier, in Figure 11, is a function of nozzle movement. The converter's output in inches of water is graphically shown as a function of nozzle movement in Figure 12. High sensitivity and consistent operation was achieved at L = 0.050" in the piezoelectric model subsequently designed and built. In this model, shown in Figure 13, the benders themselves form the movable nozzle. Static tests were made with the model, verifying its operability, using up to ± 300 volts dc for drive. Initial tests indicated very low frequency response (-3 db at 3 Hz). This should be further investigated, determined, and corrected; electrical operation of the piezoelectric benders are suspected since their required rapid dc response, high voltage mode of operation is unlike the other models discussed in this report.

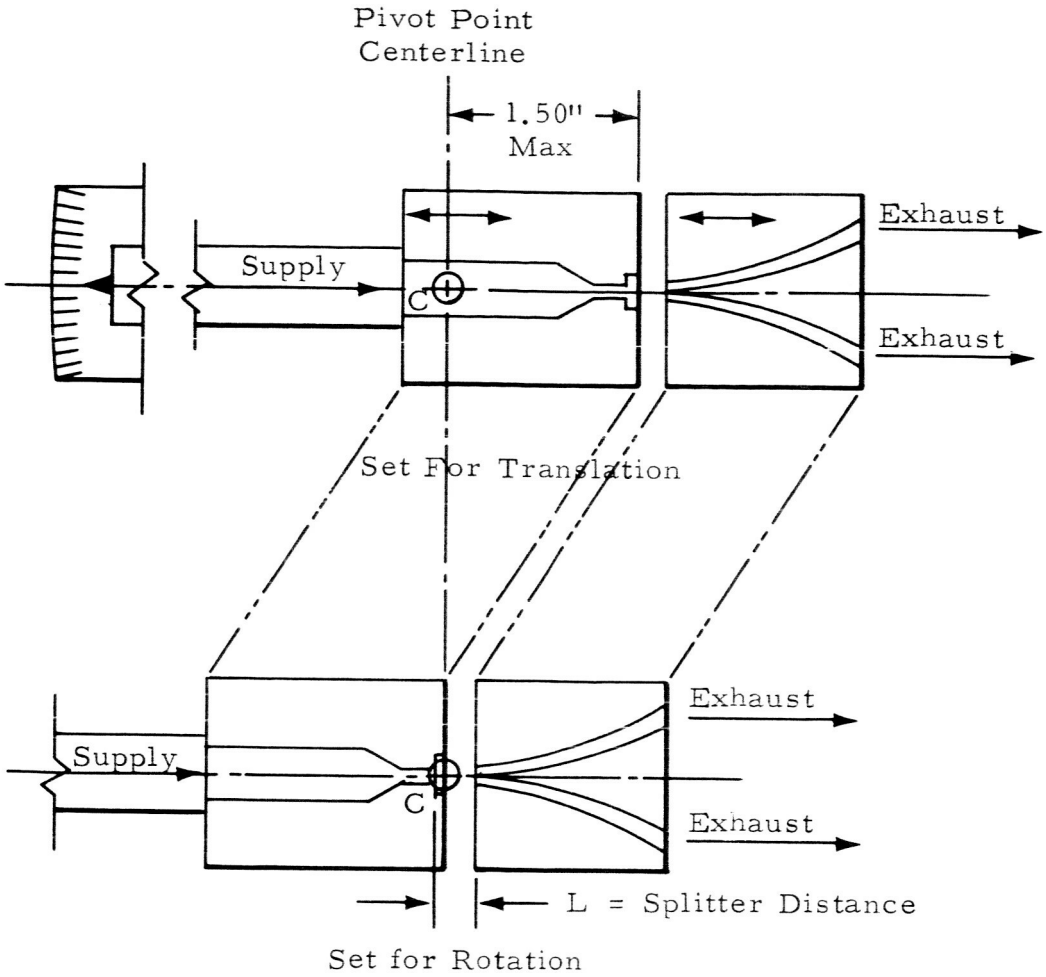

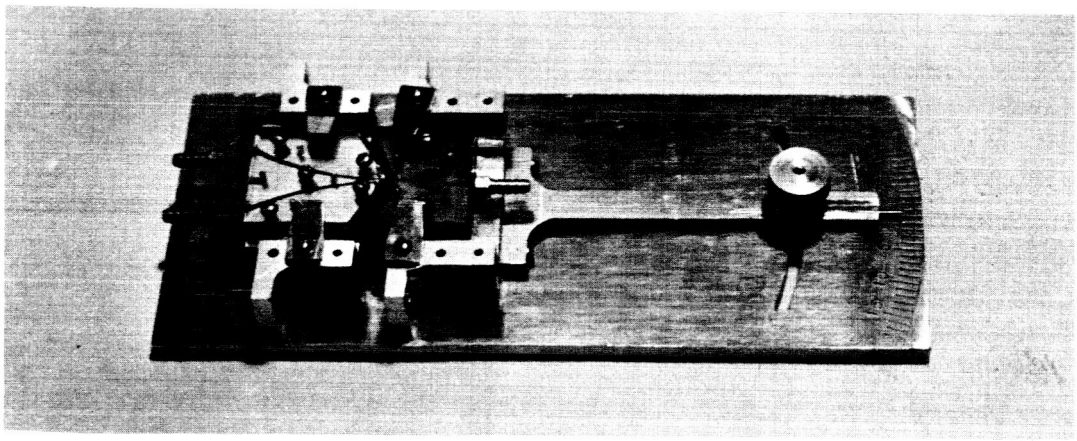

Figure 11 - Manually Driven Movable Nozzle (Schematic & Photograph)

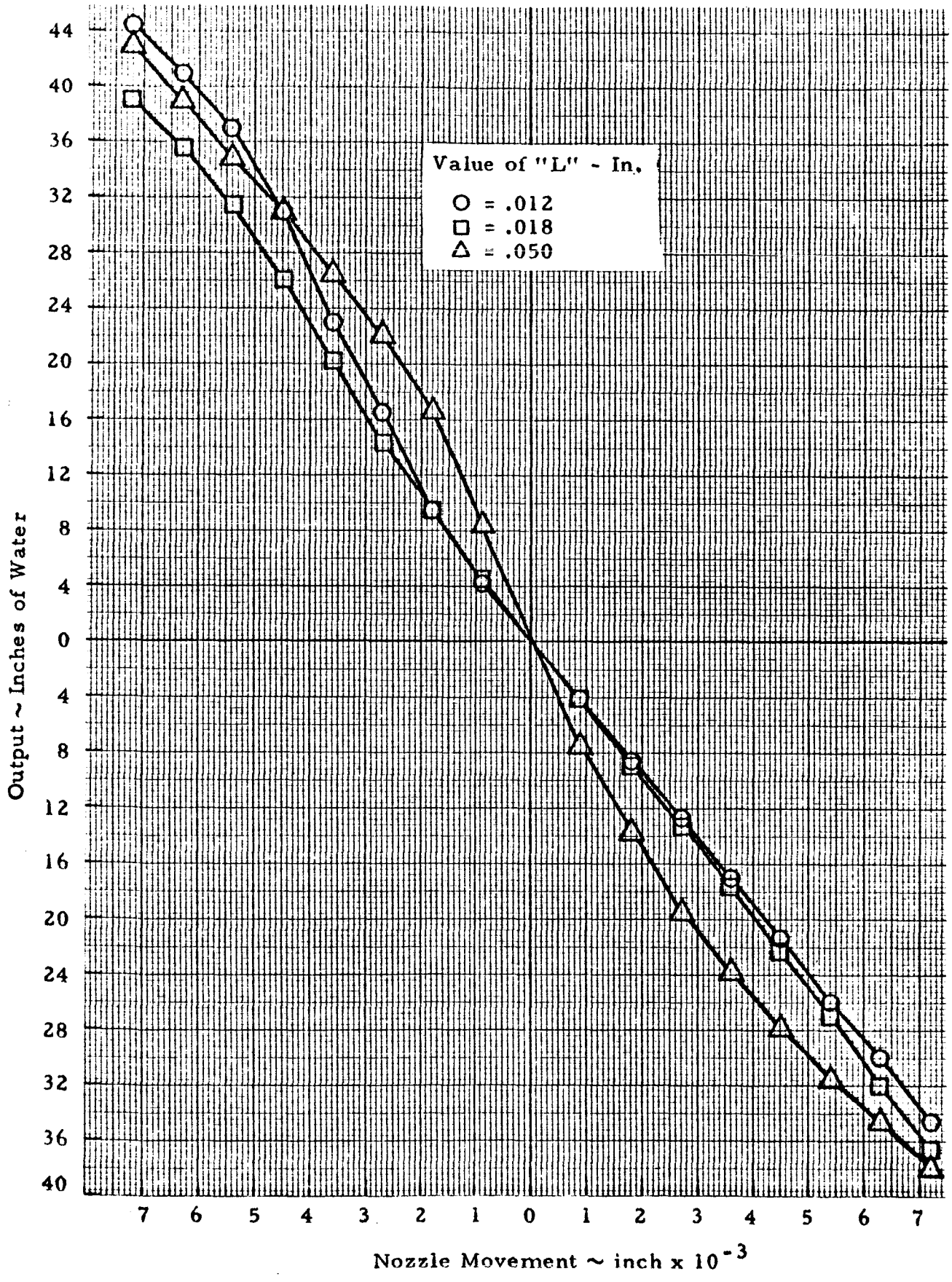

Figure 12 - Output versus Deflection - Manual Movable Nozzle Model

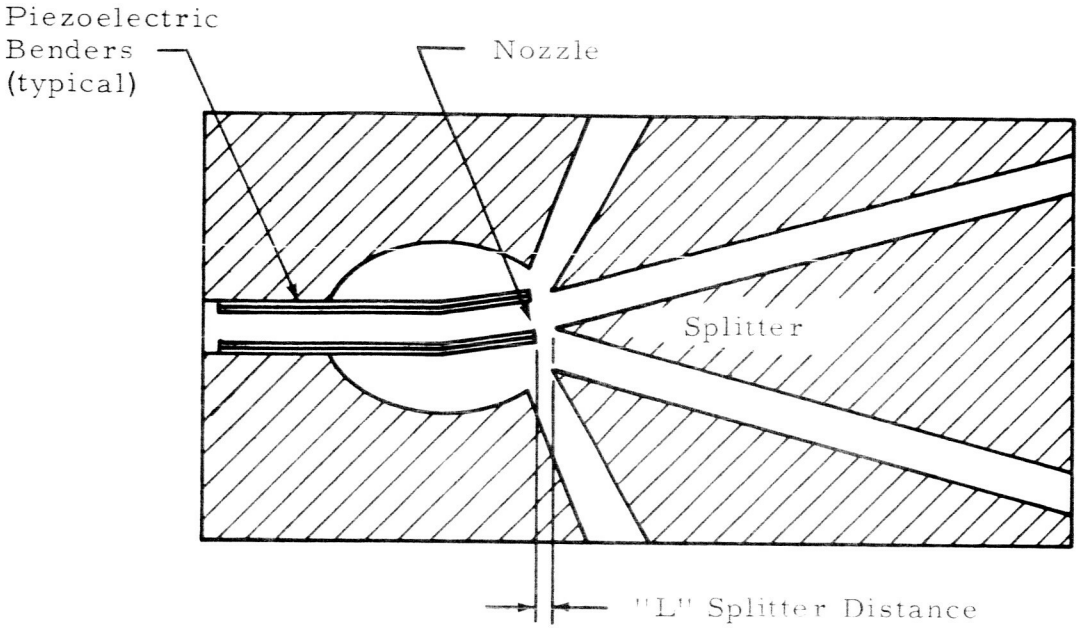

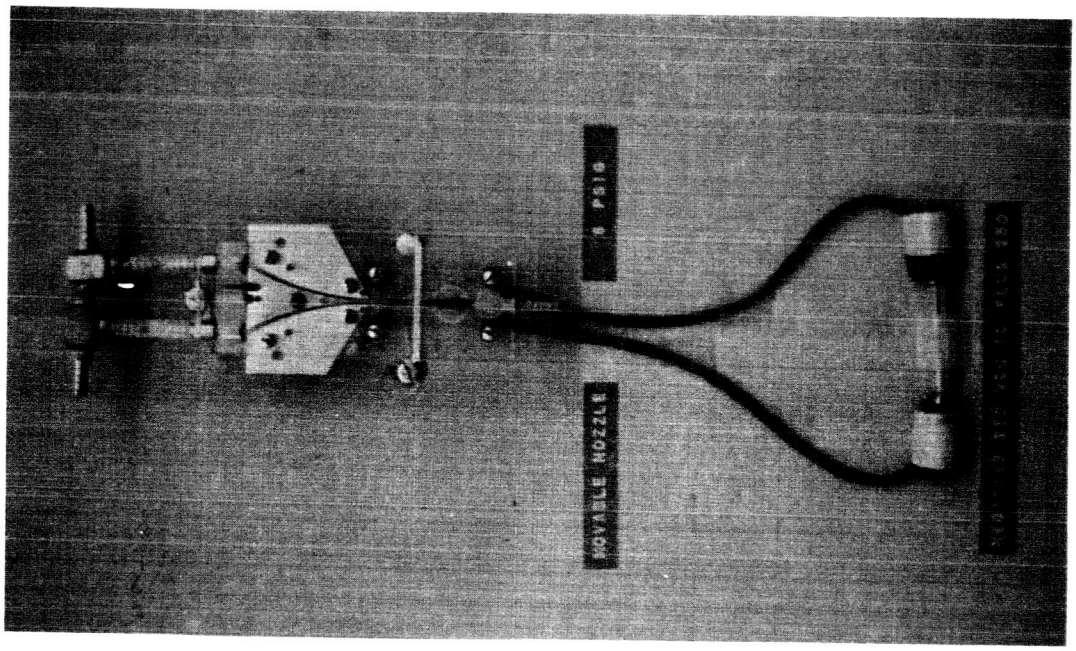

Figure 13- Piezoelectric Movable Nozzle Model (Schematic & Photograph)

6. COMPARISON OF MODELS

As discussed earlier, three electrofluid converter concepts were developed to the breadboard stage and tested. A decision was made to develop the flapper valve electrofluid converter to a prototype stage based on quantitative and qualitative comparisons between the candidate concepts. The prototype flapper valve electrofluid converter was fabricated and tested for operational characteristics. The characteristics for the flapper valve models A and B, the acoustic driver breadboard and the movable nozzle breadboard are given in Table 1.

The flapper valve shows much higher frequency response, in breadboard form (Model A), than the other two breadboards. The latest version (Model B) is designed to raise the frequency response and shows over a 50% improvement. It is felt that improvements to the filter element will raise the corner frequency appreciably.

Phase shift at the corner frequency (3 decibel power loss) was extreme for the flapper valve breadboard. This is attributable to the piezoelectric voltage deadband and the time delays and lags within the converter. Model B shows a marked improvement. It is felt that the phase shift is primarily caused by the filter acting as a damped, high order system. The absence of initial phase shift (see Figure 7) rules out measurable time delays, which were prevalent in the breadboard model.

Standby flow required by the breadboard models was quite high, particularly for the movable nozzle model. This is directly attributable to the high pressures required for reasonable system output levels and was dictated by the large internal passages within the model. The acoustic driver shows a very low standby flow because of the absence of a control or bias supply on the first stage amplifier and the relatively low pressures within the system. The bulk of the standby flow in the flapper valve electrofluid converter breadboard is from the flapper and bias supplies. These carry a flow almost twice as great as the power jet flow. Reduction in orifice sizing in Model B is primarily responsible for the 4:1 reduction in standby flow.

The values of piezoelectric drive voltage are indicative of the techniques used for developing control signal strength. The acoustic driver, as the name implies, relies on the sound pressure from a vibrating piezoelectric bender. The high voltage is required to develop mechanical energy. The movable nozzle relies on non-resonant deflection of two piezoelectric benders that are quite stiff. Again, electrical energy is required for high mechanical forces. The flapper valve, on the other hand, merely varies the impedance

Table 1

ELECTROFLUID CONVERTER OPERATING CHARACTERISTICS, BY TYPE

Operating characteristic	Converter Type: Model B Flapper Valve	Breadboard (Model A) Flapper Valve	Acoustic Driver	Movable Nozzle
Frequency Response (-3 db) – Hz	30	19	0.17	3
Phase Shift at -3 db – Degrees	-43	-142	-43	- 90
Standby Flow – Scfm	0.125	0.5	0.14	1.8
Piezoelectric Drive Voltage – Volts	60 rms*	36 rms	300 rms	±270
Output Signal at Stated Drive Voltage, – in. H_2O	22	18.5	7	27.5
Signal-to-Noise Ratio	25:1	10:1	20:1	10:1

*Square wave input, equivalent to 80 vrms sinusoidal input

across an orifice (nozzle). This requires relatively low mechanical energy, hence low voltage. The reduction in orifice size between Models A and B means that to get the same effective power from the valve, the bender has to increase the range of impedance. This, in turn, requires greater deflection, hence more energy. Both the orifice size ratio and required energy ratio are approximately 2.5:1.

Signal-to-noise ratio is primarily a function of filter design and the matching between filter and amplifier stages. The filter circuit associated with the acoustic driver converter is tuned, through component selection, to match the converter. The movable nozzle breadboard and the flapper valve models used fixed-geometry filters with the characteristics approximately matched. Filter impedances are lower than the amplifier output to reduce cross-coupling effects and prevent signal attenuation. The resulting impedance mismatch allows passage of some high frequency noise. It should be noted, however, that the unfiltered signal-to-noise ("noise" includes carrier) ratio is approximately 1:1 in the Model B flapper valve electrofluid converter.

Some of the qualitative comparisons made are in the estimation of drift, hysteresis and ease of miniaturization. Devices using amplitude modulation in the bender drive are virtually free from drift and hysteresis. Piezoelectric elements operating in a dc mode show extremely high hysteresis and develop high residual stress, resulting in creep. The movable nozzle model exhibits all these drawbacks during operation. Miniaturization of components is desirable for improvement of system response time, although output power also decreases. It is felt that reduction in size of the piezoelectric acoustic driver will reduce control signal pressure to an intolerable level. The breadboard driver presently develops a usable signal of only $\pm$ 0.1 inch of water. Signal power with the flapper valve is a complex function of valve supply pressure, flapper size and orifice size. It is felt, and subsequently proven, that an appreciable reduction can be made in the physical size of the flapper valve without sacrificing control signal pressure. Model B, overall, is approximately the same bulk as just the flapper valve assembly on the breadboard model; yet, the maximum output from the single-stage converter is 22 inches of water with a system supply pressure of 3.5 psig while Model A delivered 18.5 inches of water with a 12 psig supply.

Response Time Improvements

One major characteristic of flueric devices for control systems is relatively long response times. While the response time of an individual fluid amplifier is on the order of 0.5 to 5 msec, transport delays in the interconnecting passages and lags within cavities and filters greatly increase the response time of a flueric system over that of the basic fluid amplifier. In the following discussion, the term "delay" will be reserved for time difference between cause and effect--a distinct length of time (usually msec) as exemplified by a pressure pulse passing through a long tube; the term "lag" will mean an exponential-type effect beginning immediately after the cause (unless otherwise specified as delayed), usually defined by a time constant, as exemplified by air pressure rise in a tank which is being filled.

A primary design goal of the Model B electrofluid converter was that its response time be reduced appreciably below that of Model A. Time delays and lags of the flapper valve electrofluid converter unit are attributable to interconnections, flapper cavity size, flapper inertia, amplifier switching and diffuser length, and filters. By reducing volumes and lengths, with their resulting lags and delays, response times are appreciably improved.

The most convenient and fruitful area of work for reducing response time of the flapper valve converter is in the interconnection between the flapper valve itself and the amplifier. On Model B, this passage is greatly reduced in size and length. The next most convenient area of improvement is in the flapper valve whose internal cavity size is reduced appreciably. In conjunction with reduction in internal cavity size, a smaller flapper (bender) was designed; the resulting reduction in inertia permits better frequency response.

The next most convenient area of improvement is in the filter. By going from a simple, large volume, capacitive filter to a planar, inductive-capacitive-resistive (LCR) filter, internal volumes are reduced. It appears that transport delay through the amplifier will be the simplest means of improving system response time; this, unfortunately, is not the case. An increase above normal operating pressure causes a reduction in amplifier gain and an increase in noise and flow rates. A dimensional decrease generally gives improved response times, but a reduction in output power. Transport delay in the receiver legs can be reduced by shortening the legs and widening their diffusion angle (increase in channel width per unit length); however, the price paid for this is reduced efficiency of pressure recovery. Because of the potentially deleterious side-effects of any change, the most desirable approach to reduction of amplifier response time is determined by the intended application of the converter unit; the approach least deleterious to the intended application is chosen.

Practical information relating transport delay in the receiver legs to pressure recovery characteristics (especially efficiency), was not available. Consequently, such a program was initiated in which parametric studies on diffuser geometry can be made. The device about which this program centers is shown in Figure 14. It incorporates an air input cavity and diffuser throat of a fixed geometry. Each diffuser side pivots about centers on line with the plane across the diffuser throat, allowing each leg to be swung through a semi-vertex angle from zero to 7.5 degrees and yielding a maximum included diffuser angle of 15 degrees. Minimum diffuser length from the throat is 1.25 inches. Additional cover plates allow the effective diffuser length to be extended in increments of 0.36 inch to a full length of 2.63 inches from the throat. A movable fixture, designed to hold instrumentation probes perpendicular to the stream at the diffuser exit plane, can be translated from the diffuser centerline to the plane of the wall along a scaled line.

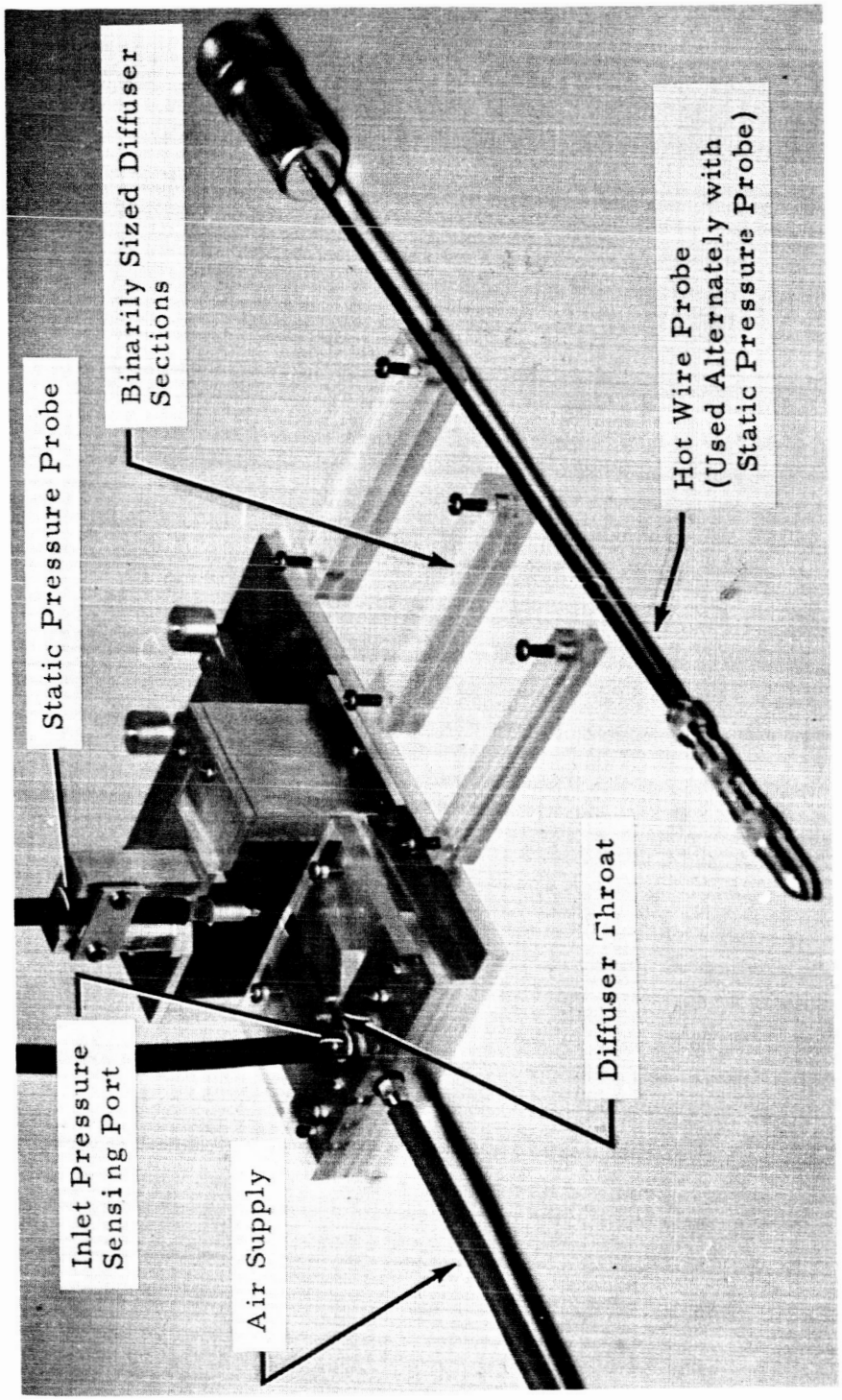

Figure 14 - Diffuser Optimization Test Device

In the planned test program, the diffuser length is set at some fixed value, the wall angles are then varied from 4 degrees to 7.5 degrees in 0.5 degree increments. Response time and pressure recovery data are taken and reduced to non-dimensional parameters for statistical analysis of conditions. One potential result of such a test program is determination of the diffuser geometry to optimize transport lag characteristics for a given pressure recovery.

Although the test program was not consummated, the model was checked out and static pressure profiles were taken across the stream. Figure 15 shows pressure profiles for various lengths of closed channel, where W = nozzle width at throat and L = downstream distance from throat to end of channel. These profiles, shown in Figure 15, indicate that for a 4° semi-vortex straight wall channel at 1 psig supply, laminar flow diffusion continues up to 33 nozzle widths downstream. Diffusion is indicated by the presence of higher pressures at the centerline than near the edges. The diffusion rate is found to be progressively smaller as downstream enclosed channel distance from the orifice increases.

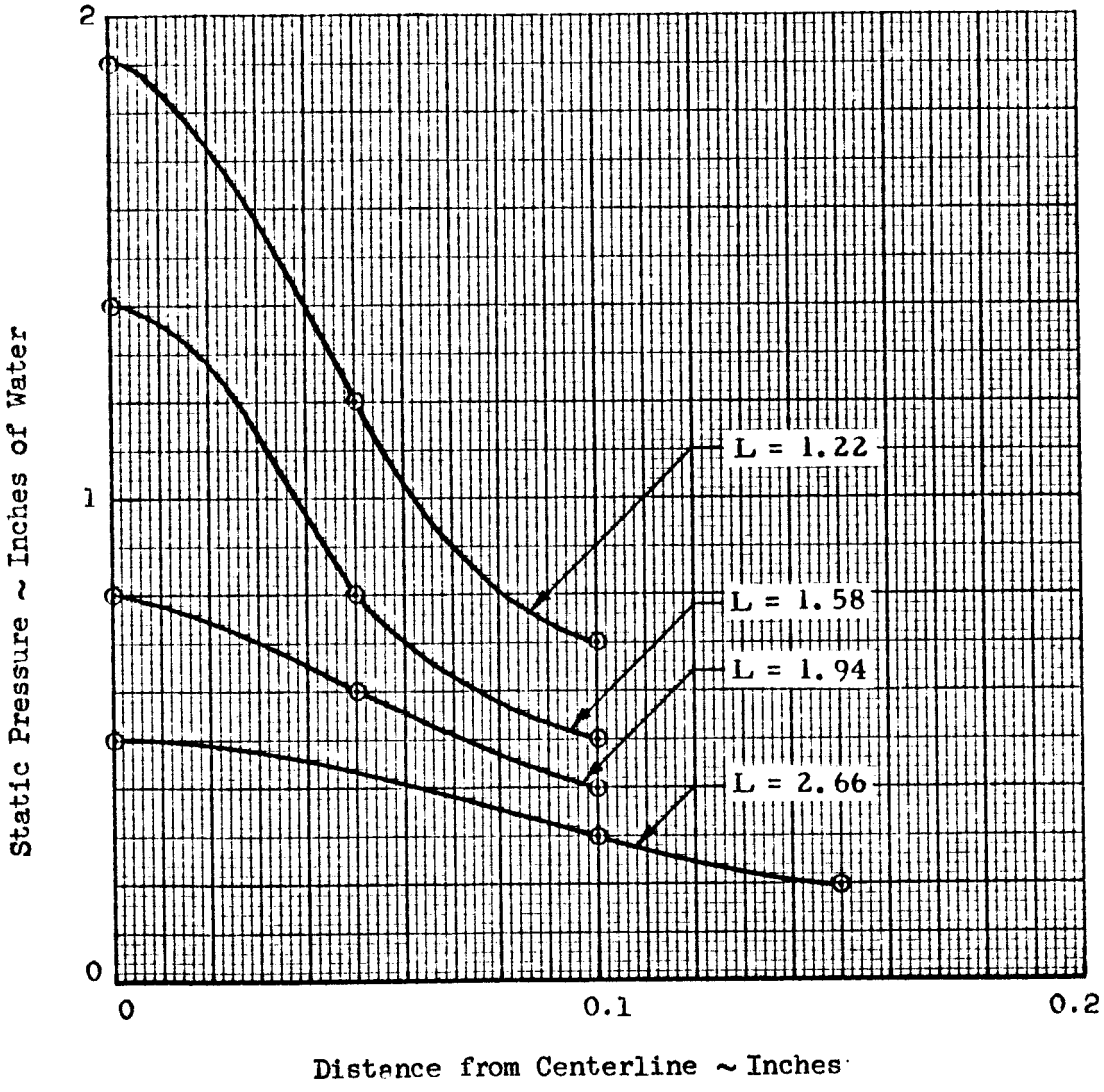

Figure 15 - Diffuser Static Pressure Profile for Lines of Constant Diffuser Length

7. ASSOCIATED DEVELOPMENT EFFORTS

During the course of developing and testing the models, various methods were developed for improving model performance. Efforts of most significance to the overall project, as well as other related areas of investigation and development, are discussed below.

Noise Reduction

The filtering problems encountered in the development of the electrofluid converter are two-fold: the primary requirement is to eliminate high-frequency noise, the secondary requirement is to reduce the carrier frequency at the output. It is necessary to meet these requirements without incurring attenuation of the direct output. Filter development usually follows empirical lines, although initial direction is determined by analog electrical, acoustic or delay-line theory.

When the original prototype flapper valve electrofluid converter was being developed, the high noise level of the output signal showed that it is desirable to use a filter. A simple orifice was tried first and then discarded because of the attenuation of the output signals. The filter configuration next considered was that of a chamber or "drum". Behavior of a chamber is analogous to that of a capacitor, where chamber pressure rise time is a function of chamber volume and outlet orifice size. By treating the outlet orifice as a short tube, the resistance to flow is proportional to the length and inversely proportional to the fourth power of diameter. The inductive reactance of the "orifice" is proportional to the product of length and frequency and inversely proportional to the square of the diameter. The size (diameter and length) of the output "orifice" then determines the attenuation of noise since the inductive reactance acts as a resistor, over the above pure fluid resistance, as a function of frequency. The lower frequency (below 1 KHz) generated by the resonating piezoelectric bender is reduced by the capacitive reactance of the chamber. Capacitive reactance is inversely proportional to the product of frequency and volume. Additional reduction of the flow frequency signal is accomplished by sizing the chamber volume such that the pressure rise time is approximately the reciprocal of the signal frequency, in radians per second. Cavity pressure is then about 180° out of phase with signal pressure, achieving cancellation of the pressure fluctuations.

The cylindrical drum filter presently used has an internal diameter of 0.625 inches and a length of 0.258 inches between ends. Input is a standard fitting, 0.090 inches ID, and the output is a 0.026 inch ID tube approximately 0.10 inches in length. High frequency noise is completely eliminated with this filter and the resonant frequency amplitude is reduced by approximately 90%.

The effectiveness of the "drum" filter is enhanced by the axial alignment of input and output ports with their axes parallel to the cylindrical axis. This configuration gives a desirable wave interaction within the cavity, since having the ports unaligned or set with their axes perpendicular to the chamber axis reduces the low frequency attenuation to approximately 70%. The "drum" filter is particularly effective above 700 Hertz (90% amplitude reduction) with the effectiveness decreasing with lower resonant frequencies (50% reduction at 250 Hz).

Concurrent with the development of the acoustic driver electrofluid converter, a model of a low-pass filter was developed. This filter is roughly analogous to an electronic LCR filter. The three major components of this filter are an inductive accumulator, a capacitive chamber, and a by-pass restrictor. The small volumes within this filter make it approximately 0.0075 seconds faster than the "drum." Another distinct advantage of this configuration is its adaptability to a planar form. A planar LCR filter, as shown in Figure 16, is relatively easy to fabricate, photochemical etching or chemical milling being applicable.

The LCR filter should be closely "tuned" to the particular amplifier with which it is to be employed. The LCR filter may be approximated by a network of four volumes and four resistors as shown. Volume 1 is the line volumes from the filter input to the orifice plane of Volume 3, the entrance plane to Volume 2, and the narrowest part of the fluid resistor, R_{14}. Volume 4 is line volumes from the exit orifice plane of Volume 3 to the filter output and from R_{14} to the filter output. Notation for analysis shows the direction of flow in the subscripts: R_{14} is the resistor between Volumes 1 and 4 and the associated weight flow is I_{14}. Flow through resistors may be considered as isentropic. Flows within the volumes may be either isentropic or isothermal, depending on flow rates. With low velocity flow within a volume heat can freely flow from the fluid to the volume walls. The flow process then will be isothermal, fluid temperature equaling wall temperature. With high flow rates the process approaches isentropic behavior because the "thermal inertia" of the fluid/wall interface prohibits high rates of heat transfer. Most flow processes are polytropic, being neither isentropic nor isothermal but somewhere in between. The dimensions of the LCR filter, X-FCR-002-2, were arrived at by preliminary calculation of capacitive reactance for desired volumes and of fluid resistance and inductive reactance for the resistors and passages. Estimated pressures and flows for the Model B electrofluid converter were taken for these calculations.

The X-FCR-002-2 filter, used with the full size amplifier in Model B, reduces the amplitude of the carrier frequency from the flapper valve by 85 to 90%, depending on the flow range. As expected, the filter operates better with higher flow rates (increased resistivity). The dc signal component is passed without attenuation over a very wide range of flows. Effectiveness falls off quite rapidly with decreasing frequency (reduced inductive reactance); the attenuation of an alternating amplitude at 243 Hz is approximately 30%.

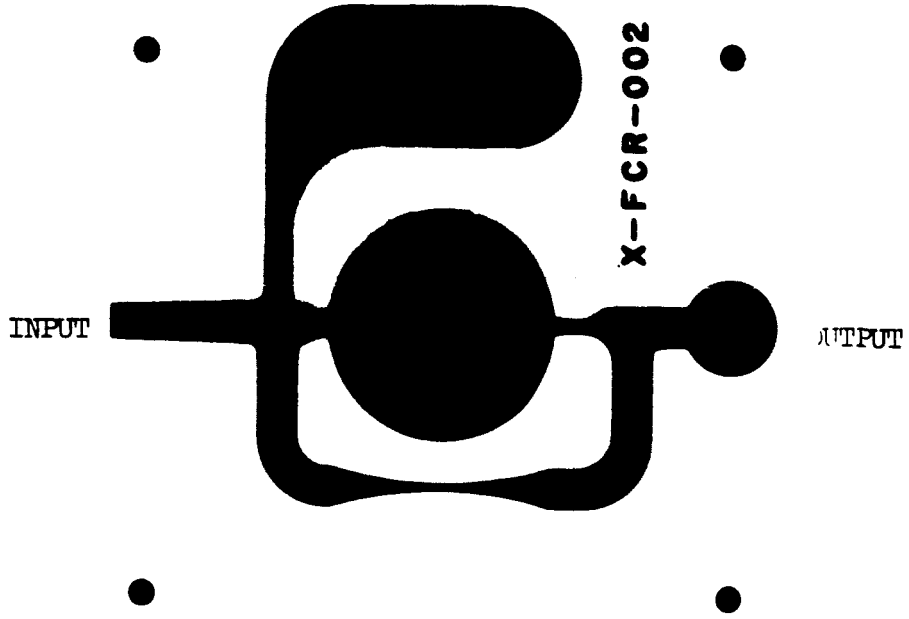

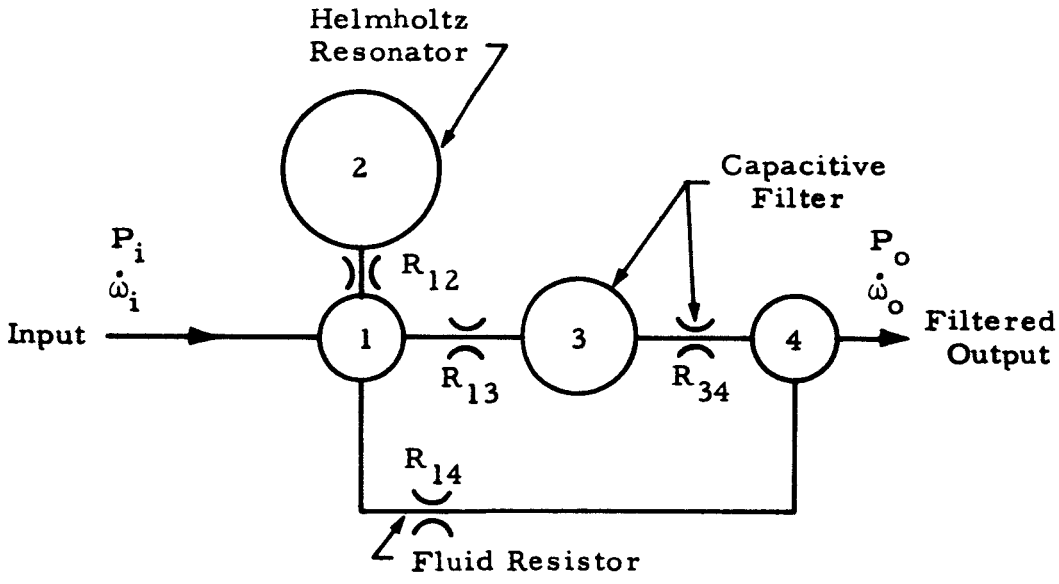

Filter System Circuit Schematic

Figure 16 - Planar Filter Type LCR Master (4X) Silhouette & Schematic

Figure 17 is an oscillograph trace of input voltage and output pressure from the integrally-packaged, flapper-valve electrofluid converter without a filter. The carrier frequency of 1100 Hz passes through quite clearly and is almost inseparable from the system noise. Figure 18 is a composite picture taken from oscillograph traces of input voltage and output pressures with a "drum" filter and a planar LCR filter. Input was modulated at 10 Hz. The composite picture was taken with the output oscilloscope beam synchronized with the input signal. The relative phase shifts evident between outputs and input signals are valid, since the beam sweep of the output traces was triggered by the rise of the input trace voltage above zero volts. It should be noted that the "drum" filter is general purpose, the -20 db point occurring at approximately 800 Hz, and the X-FCR-002-2 filter was tuned, approximately, to 1100 Hz and slightly higher flow rates than the Model B electrofluid converter developed.

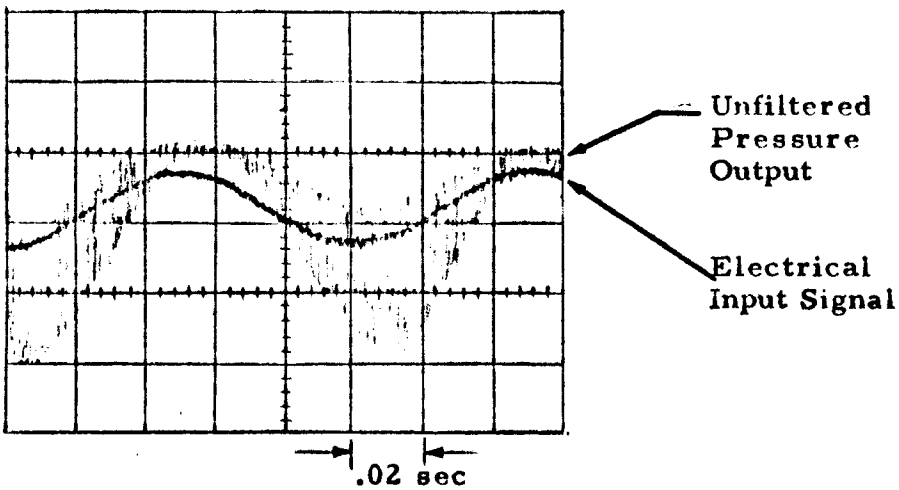

Figure 17 - Unfiltered Pressure Output and Electrical Input vs Time

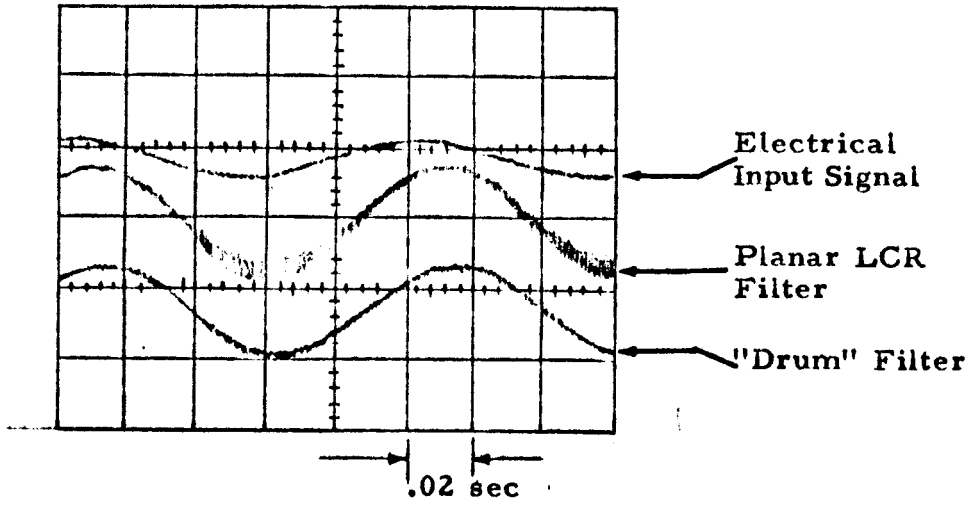

Figure 18 - Comparison of LCR and "Drum" Filters (Oscilloscope Photo Tracing)

8. RECOMMENDED FUTURE WORK

Specific recommendations in conjunction with the general conclusions are given in the following paragraphs.

Configuration Improvement

General configuration improvements are readily possible in the deflectable splitter, flapper valve, acoustic driver, and movable nozzle configurations. They should include better sealing, shorter interconnection, and simpler packaging. Initial life and temperature tests should be made. Other improvements unique to each model and specific work which should be done on each model are presented below.

Deflectable Splitter: Some studies of the deflectable splitter, using flow visualization, should be made to determine the practicality of this approach. The MSFC/Astrionics Laboratory polarized-light water table might be used for initial studies. Several splitter nose shapes should be tested to optimize sensitivity through a range of deflection achievable by piezoelectric motivation. If such a study proves that the deflectable splitter principle is practical, further development in packaging will be necessary, especially since a moving part with a flexible fairing must be sealed deep within the unit.

Flapper Valve: Since the present device, Model B, is designed for planar etching, a planar-etched model incorporating a layout fully integrating the flapper valve case, the fluid amplifier, all restrictors, and interconnecting channels should be made and fully tested. Further development of the biased fluid amplifier, with and without its filter, should be performed. When a satisfactory configuration is developed, it should be built in fully integrated form as the Model B. Highly durable flapper bearing material for the flapper-nozzle interface should be found and proven. Oppositely poled piezoelectric pieces should be installed after being externally tested. A configuration employing one input nozzle to each face of the bender with a single cavity exit should be investigated; a single flapper would thereby operate on two nozzles. Goals of amplifier development toward matching would be unchanged. A higher level of converter performance would be expected over the existing single-nozzle design.

Acoustic Driver: Development is necessary to increase the power output of the acoustic driver. Advantages of the cantilever bender versus diaphragm type as the active element should be investigated and the better one developed. The developmental progression of amplifier and filter optimization, using semi-integrated packaging and finally integrated packaging, should next be pursued.

Movable Nozzle: Improvements suggested when the last model was being assembled, especially in the installation of the piezoelectric benders, should be implemented in a modification of this design. A method of tying the bender tips together should be developed for added stability. The shortest cantilever design commensurate with good performance should then be determined to minimize mechanical bender resonance due to externally induced vibrations along the cantilever's sensitive axis, i.e., normal to the bender plane. Electrical feedback from a pressure pickoff to increase accuracy and stability should be studied and implemented.

Diffuser Optimization Test Device

This device may be used for a multiplicity of purposes. Its primary purpose is for parametric investigation of diffuser lengths and angles to optimize the transport lag and pressure recovery characteristics. This design data, subjected to scaling, would serve for advanced diffuser designs in special-purpose amplifiers. This device may also be used for determining duct loading effects through partial blockage of the passage. Additional work should be performed to glean information on turbulence transition in diffusers, boundary layer stability, turbulent and laminar boundary layer phenomena in diffuser lengths, and velocity profiles through expanding rectangular sections. A preliminary test plan is presented in the body of this report.

Electromechanical Motivation

Two areas of electromechanical motivation are of interest for further study, piezoelectric and magnetostrictive.

During the course of study of piezoelectric devices, one area requiring further investigation was suggested by the frequency response tests that were performed. This is the electromechanical bender. Frequency response of the motivation device itself needs further study while operating in its pressure environment within the flapper cavity. If this frequency response were known, it would be the upper limit of system performance and would therefore indicate whether improvement in the resonant member or chamber and nozzle would be required for system improvement. Such frequency response data could be acquired by electrical contact or visual techniques. Investigations of frequency response should be made with supply pressure, frequency, bender shape, and contact materials as variables.

Other experiments to establish practicality of using a single layer piezoelectric diaphragm instead of cantilever laminate as a flapper would be valuable. One such diaphragm study has already been mentioned.

Power measurements, both electrical input and mechanical output, would give valuable insight into the level of efficiency attained. The study would also serve to guide designers of complementary electronics equipment and establish whether the power level required by the crystal per se is of sufficient magnitude to warrant studies in its reduction.

Other Means of Carrier Frequency Generation

The successful application of the amplitude modulation principle using piezoelectric benders opens the door to possible usage of other means of generating the pneumatic carrier signal. Magnetostriction and pulling-gap, proportioned relays are two typical principles which are suitable for this purpose.

While hysteresis, temperature sensitivity and excessive power requirement ruled out alternating proportional mode of operation with magnetostrictive materials, they do not represent particularly difficult problems if amplitude modulation operation is used. Magnetostrictive devices having the capability of operation in environments at much higher temperatures than the piezoelectric materials should be seriously considered for hot gas control systems.

Pulling-gap electromagnetic relays have been extensively used in servovalve applications. It has been found, however, that the small magnetic gaps essential to proper operation can trap magnetic dust in the fluid medium being controlled and that over 90% of servo valve reliability problems in the past can be traced to clogged magnetic pulling gaps. To generate an ac carrier signal in a gas, however, the magnetic gap size can be considerably enlarged (from a few thousandths of an inch to hundredths of an inch) such that the reliability of the signal converter can be considerably increased.

A magnetic signal converter is usually made of free-machining, ferromagnetic materials, an advantage over the piezoelectric ceramics which can only be ground or lapped if any degree of precision is required.

Based on these considerations it is recommended that further study effort be directed in the area of generating pneumatic carrier signals by magnetic or magnetostrictive methods.

Pulse Duration Modulation

The modulation methods previously discussed include Pulse Duration Modulation (PDM). It offers important advantages as an electrofluid conversion technique because drift and non-linearities such as hysteresis, creepage, and temperature variations do not affect the response. Neither does moderate variation of supply pressure if the output is used to drive a digital element.

Four possible configurations of PDM should be investigated. Each configuration progressively uses more of the functional blocks of Figure 19.

Case	Electrical Input Signal	Fluid Output Signal
I	Digital (PDM Pulse Train)	Digital (PDM Pulse Train)
II	Digital (PDM Pulse Train)	Analog
III	Analog	Digital (PDM Pulse Train)
IV	Analog	Analog

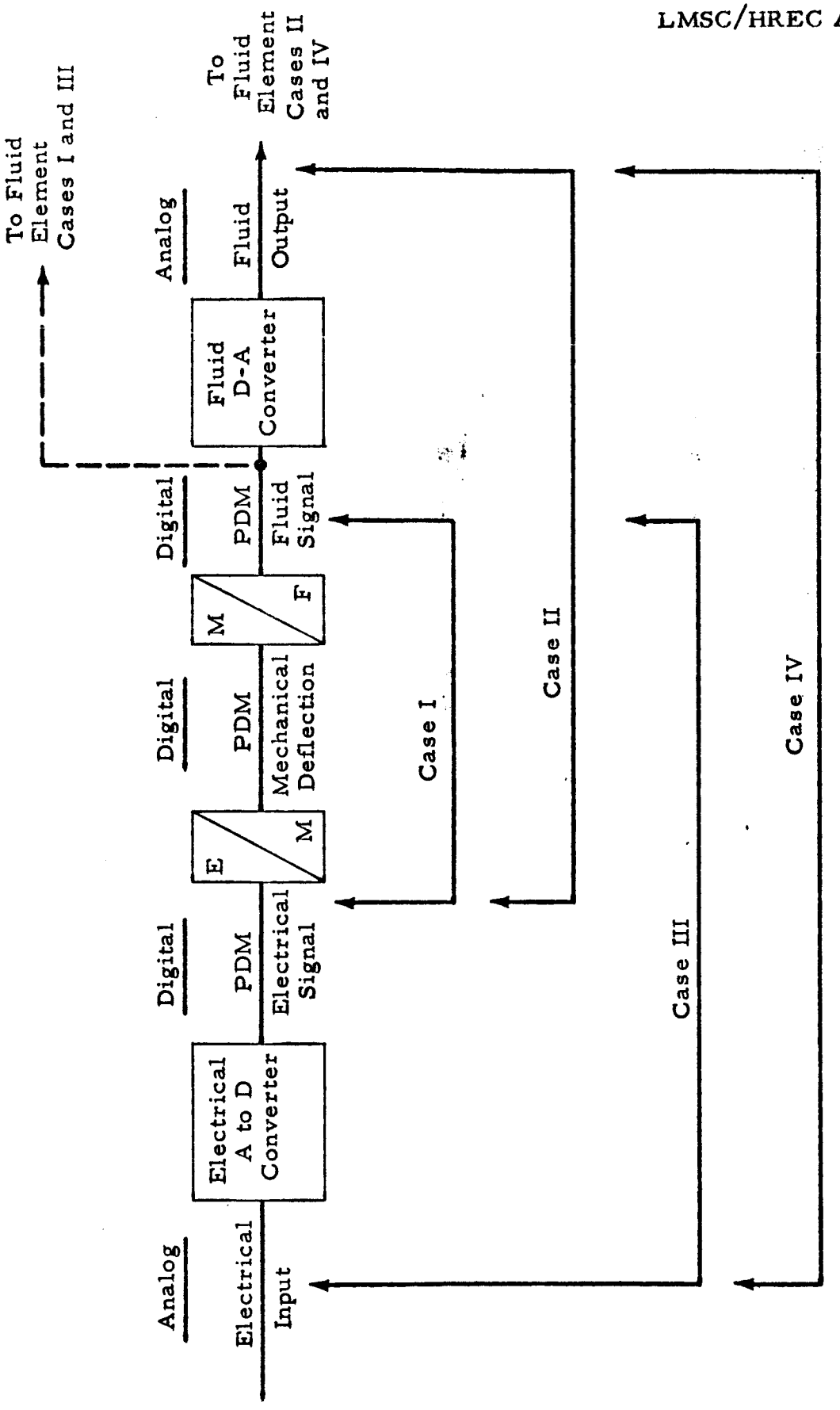

Figure 19 - Pulse Duration Modulation, Functional Diagram

It is assumed here that the proportional input signals of Cases III and IV are converted to electrical PDM pulse trains by electrical circuits before they are fed into the electrofluid converter, thereby providing higher accuracy, faster response, and a smaller package than pure fluid A/D conversion. Hence, this investigation could be restricted to Cases I and II with electrical bistable input signals.

Simple on-off components could be used. However, initial studies of feasibility should be done on the movable nozzle model discussed previously, as shown in Figure 20. Plenum and/or filters would be introduced for development early in the studies if proportional (instead of PDM) fluids output is required. The proportional output is obtained by the time averaging of output pressures. By appropriate plenum sizes and outlet orifices, the difference, ΔP of the plenum pressures will be proportional to the electrical PDM input signal dc component.

Further development of PDM beyond the initial phase would probably center around bistable amplifiers for more positive switching to fixed levels. Switching times in the 1/2 to 1 millisecond range are typical for bistable amplifiers, indicating that high enough pulse rates are feasible.

Should any system requirements be incompatible with piezoelectrics, magnetic switching might be investigated. One possible arrangement is shown in Figure 21.

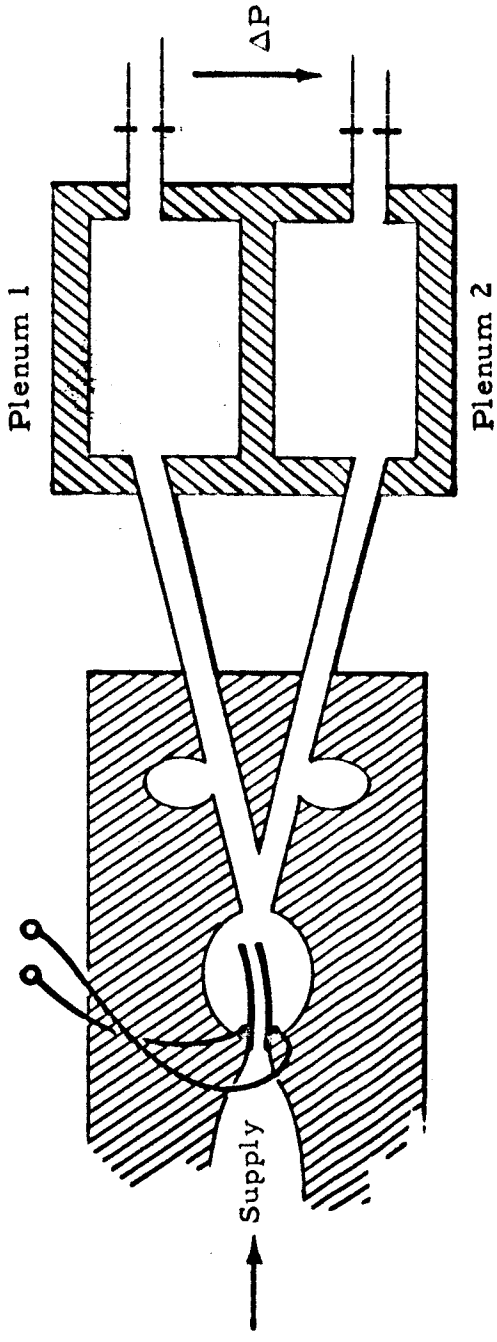

Figure 20 - Configuration for Time-Averaging Fluid PDM Signals

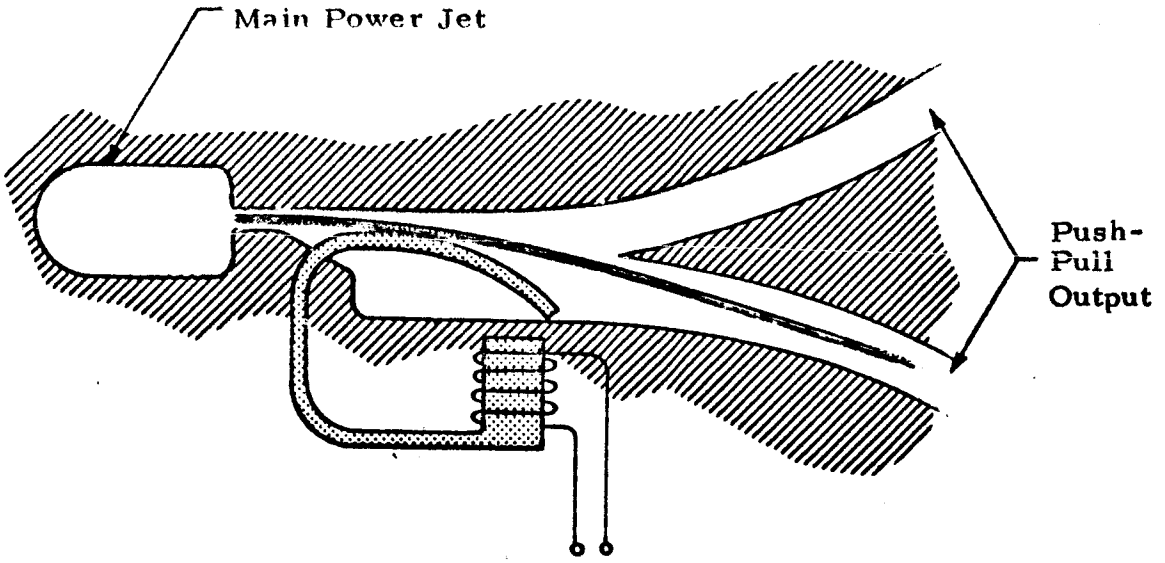

100% Signal

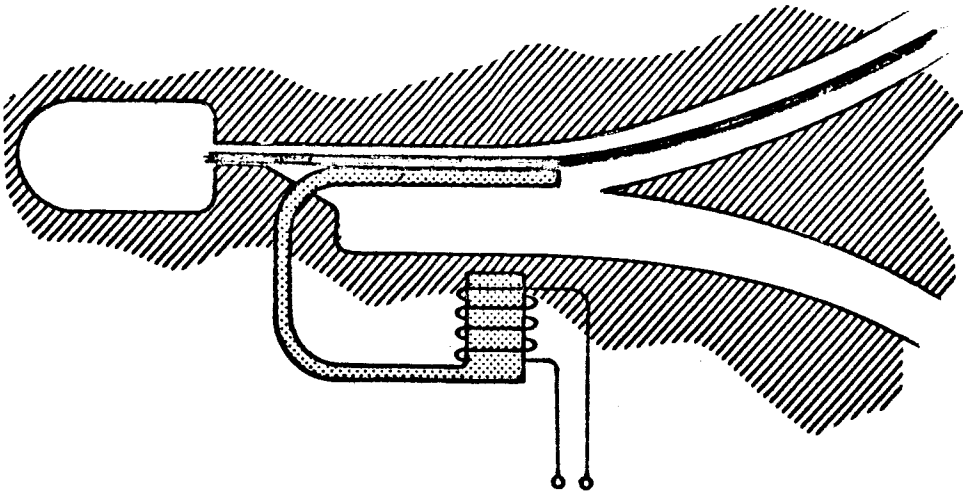

Signal OFF

Figure 21 - Magnetic Motivation of Bistable Switching

9. BIBLIOGRAPHY

1. Humphrey, R. L. and F. M. Manion, Bowles Engineering, "Low-Pass Filters for Pneumatic Amplifiers," Proceedings of the Fluid Amplification Symposium, May 1964, Vol. I., Harry Diamond Laboratories, Washington, D. C.

2. Gottron, R. N., Harry Diamond Laboratories, "Noise Reduction by Jet-Edge and Resonator Coupling," Proceedings of the Fluid Amplification Symposium, May 1964, Vol. I, Washington, D. C.

3. Verdernikoff, A. N., An Experimental Investigation of the Flow of Air in a Flat Broadening Channel, NACA Technical Memorandum, No. 1059.

4. Kline, S. J., D. E. Abbott and R. W. Fox, "Optimum Design of Straight Walled Diffusers," Transactions of the ASME, Vol. 81, (1959) Series D, No. 3, pp. 321-331.

5. Remmler, K. L., et. al., Summary Report, Fluid Control System Study, Technical Report HREC/1480(Z)-1, LMSC/HREC A712471, 7 December 1965.

6. Floyd, G. O., et. al., Final Report, LMSC/HREC Fluidic/Flueric Independent Development, 1965 (to be published).

APPENDIX A

ANALYSIS OF PIEZOELECTRICAL ELEMENT MECHANICS

Initial studies of piezoelectrics revealed problems of non-linearities; the worst of which are creepage[1] and hysteresis. Practical design considerations demanded that the extent of these problems be well known within the limitations of their use for electrofluid converters. Only then could fluid passages, chambers, etc. be practically designed.

Information from vendors provided no useful information on hysteresis or creepage, but did provide the modulus of elasticity and piezoelectric constants (deflection per volt). These values permitted bender deflection to be calculated, providing valuable initial guidelines for design. Such calculations are:

- <u>Deflection or Gain</u>

The bending moment, M, in a piezoelectric material of thickness 2t (inactive zone of center strip neglected) under a driving field of voltage e is

$$M = Y \left(d \quad \frac{e}{2t}\right) w\, t^2 \qquad \text{(newton-meters)}$$

where:

Y = modulus of elasticity, newtons/meter^2,

d = piezoelectric constant, meters/volt,

w = width of bender, meters.

1. "Creepage" is defined as continued physical change after voltage has ceased to change.

Substituting this expression into the equation for the bending of beams yields

$$\frac{d^2z}{dx^2} = -\frac{M}{Y\ I_{yy}} = -3\,d\ \frac{e}{(2t)^2}$$

where I_{yy} = moment of inertia about the axis orthogonal to x and z axes.

For cantilever mounting, $z = \frac{dz}{dx} = 0$ when $x = 0$, the integration yields the gains

$$\left(\frac{\delta}{e}\right)_{series} = \frac{3}{2}\,d\ \frac{L^2}{(2t)^2} \tag{1a}$$

$$\left(\frac{\delta}{e}\right)_{parallel} = 3\,d\ \frac{L^2}{(2t)^2} \tag{1b}$$

when benders are connected as shown in Figures 1a and 1b respectively

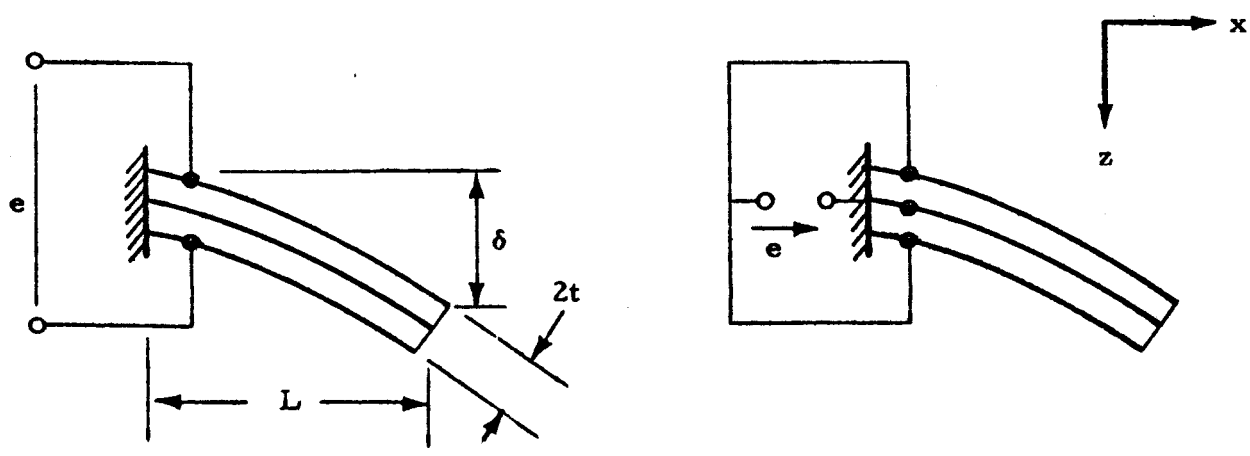

a. Series Connection

b. Parallel Connection

Figure 1 - Electrical Connections for Benders

APPENDIX B

OPERATING INSTRUCTIONS
LOCKHEED/HREC ELECTROFLUID CONVERTER, MODEL B

1. GENERAL

The breadboard model of the Lockheed/HREC electrofluid converter is mounted on an electronic control chassis which provides electrical inputs to the model to demonstrate its capabilities. The following instructions describe how to adjust and operate the control chassis when using only the chassis internal electrical inputs or adding an external electrical input to operate the converter. To prevent damage to piezoelectric bender, these instructions should be strictly observed.

2. TECHNICAL DATA

2.1 Chassis Power - 115 Volts, 60 Hz

2.2 Supply Pressure - 4 psig maximum

2.3 Maximum External Input Signal - $\pm$ 0.75 volts

3. OPERATION BY CHASSIS CONTROLS

3.1 Turn gain control full CCW.

3.2 Connect ac voltmeter (set on 100 volt range) across high voltage monitor terminals.

3.3 Switch modulator control switch to the left.

3.4 Turn dc bias internal control full CCW.

3.5 Switch power control to ON position.

3.6 Turn ac bias control full CW.

3.7 Turn gain control CW until voltmeter reads 60 volts.

3.8 Adjust frequency control: (a) to the resonance frequency of the piezoelectric bender when minimum pressure is observed; then (b) decrease the frequency by turning the control CW until the output pressure (P_o) starts to increase.

3.9 Turn dc bias control CCW until maximum P_o occurs, then turn ac bias control CW until P_o starts to decrease.

3.10 Turn gain control full CCW.

3.11 Turn dc bias internal control full CW.

3.12 Adjust gain control until voltmeter reads $\pm$ 70 volts.

3.13 Repeat steps 3.9, 3.10, 3.11, and 3.12 until desired ac bias setting is correct (3.9).

3.14 Turn dc bias internal control to manually vary P_o.

4. OPERATION BY EXTERNAL SIGNAL

4.1 Complete steps 3.1 through 3.13.

4.2 Turn dc bias internal control full CCW.

4.3 Switch modulation control to the right.

4.4 Connect external input electrical signal (maximum 1.5 pp volts) to the external GR jacks; signal ground to the black jack and voltage signal to the red jack.

4.5 If the input signal becomes negative, adjust the dc bias internal control until the internal ground (green) jack has a voltage slightly negative to input signal ground.

4.6 Adjust gain until voltmeter across high voltage monitor reads 140 pp volts. The output pressure P_o will now vary as a function of the external input signal.